NASA CONTRACTOR REPORT

NASA CR-648

NASA CR-648

ELECTROLYSIS CELL FOR ORBITAL TEST

by C. W. Fetheroff, R. G. Huebscher, D. L. DeRespiris, J. G. DeSteese, and G. L. Mrava

Prepared by
TRW INCORPORATED
Cleveland, Ohio
for

NATIONAL AERONAUTICS AND SPACE ADMINISTRATION • WASHINGTON, D. C. • NOVEMBER 1966

NASA CR-648

ELECTROLYSIS CELL FOR ORBITAL TEST

By C. W. Fetheroff, R. G. Huebscher, D. L. DeRespiris,
J. G. DeSteese, and G. L. Mrava

Prepared under Contract No. NASw-998 by
TRW INCORPORATED
Cleveland, Ohio

for

NATIONAL AERONAUTICS AND SPACE ADMINISTRATION

For sale by the Clearinghouse for Federal Scientific and Technical Information
Springfield, Virginia 22151 – Price $2.50

ABSTRACT

Detailed studies were made of the processes occurring at the electrodes of compact water electrolysis cells under varying conditions of operation. Based on these studies, two identical water electrolysis subsystems, including complete analytical instrumentation and a water supply for 24 hour's operation, were designed and fabricated. The wick-vapor-feed concept, requiring no dynamic components, was utilized. Each of the two flight packages weighs 14.5 lb. During the Performance Acceptance Test an average voltage of approximately 1.65 volts per cell at a current density of 100 amperes/square ft was obtained at an average cell temperature of approximately 93°F. The two units were delivered to NASA for additional laboratory testing prior to an orbital test to determine the effects of gravity-free operation on water electrolysis subsystem performance.

TABLE OF CONTENTS

LIST OF FIGURES

LIST OF TABLES

ELECTROLYSIS CELL FOR ORBITAL TEST

by C. W. Fetheroff, R. G. Huebscher, D. L. DeRespiris, J. G. DeSteese, & G. L. Mrava
TRW Inc.

SUMMARY

Future spacecraft environmental control systems will require high performance water electrolysis subsystems. It will be essential that these subsystems deliver high purity gases, free of electrolyte entrainment, with a high degree of reliability.

Prior to the work under this contract, TRW had demonstrated the capability to fabricate compact, lightweight, highly efficient electrolysis cells, both on in-house programs and under government contract. Moreover, at least in a laboratory environment, these cells had been shown to be capable of delivering gases free of any electrolyte entrainment without the need for any external components to achieve phase separation.

The objective of the work under this contract was to design and fabricate two water electrolysis subsystems, complete with instrumentation, suitable for orbital test. The purpose of the orbital test will be to determine what differences, if any, exist between the performances of the electrolysis cell subsystem under actual gravity-free conditions and under normal laboratory conditions. Of particular interest during this test will be the determination of whether phase separation at stationary electrolysis cell electrodes is feasible in the absence of external force fields.

The scope of the work accomplished under the contract encompassed definition of the orbital experiment, development of the instrumentation required to monitor subsystem performance in orbit, design and fabrication of two identical flight packages, and demonstration of subsystem performance during a continuous 24-hour run on one unit. The units were subsequently delivered to NASA for additional performance testing and environmental testing.

During the experimental definition phase of the program, detailed studies were made of the processes occurring at the electrodes under varying conditions of operation. These studies included direct visual observations of the electrode processes on experimental preprototype cells with transparent end-plates. Correlations were drawn between the physical and chemical phenomena observed, the cell and subsystem configurations, the operating parameters and the cell performance. On the basis of these studies the specifications, configurations and data requirements were formulated for the flight units.

Each of the flight units contains a three-cell electrolysis stack with an integral wick-vapor-feed system, a water reservoir containing sufficient water inventory for operation for at least 24 hours in orbit, complete analytical instrumentation, and electronics for signal conditioning. Instrumentation was provided to measure cell temperature, cell voltages and current, gas temperatures, gas humidities, gas pressures, gas flows, any contamination of either effluent gas stream by the other gas, the water supply system pressure, and two stages of electrolyte entrainment detection in each effluent gas stream. Weight of each of the flight packages is approximately 14.5 lb.

A continuous 24-hour performance run was conducted on one of the two flight units. The unit was started at ambient laboratory temperature, approximately simulating an orbital startup. Due to convective losses to the laboratory atmosphere, however, cell temperature reached a maximum of approximately $98^{\circ}F$ during the test. Despite the low temperature, the average of the three cell voltages for the 24-hour period was approximately 1.65 volts. Cell current was held constant at 6.25 amperes (100 amperes/square foot) for the entire test. Improved performance is expected at the $140^{\circ}F$ design temperature for the orbital test.

It has been verified that simple, compact, lightweight, and highly efficient electrolysis cell subsystems containing no dynamic components can be fabricated for the environment anticipated in space vehicles. It is expected that further testing will show no degradation in performance under gravity-free conditions or due to launch stresses. The design of the hardware is such that it may be directly scaled in size for any desired capacity. A minor modification in the water reservoir would be required for connection to an external water source for extended operating periods.

1.0 INTRODUCTION

Spacecraft environmental control systems for long duration missions will require regeneration of oxygen from carbon dioxide. The most probable methods for accomplishing this task involve reduction of the carbon dioxide with hydrogen to form water. The water produced is then fed to an electrolysis cell to form hydrogen, which is returned to the reduction unit, and breathing oxygen. It is essential that the water electrolysis unit be capable of supplying high purity gases, free of electrolyte entrainment, in a gravity-free environment.

TRW has been working on the development of compact, lightweight, highly efficient electrolysis cells for the above application. Unlike conventional electrolysis cells, which pose a phase separation problem in a gravity-free environment, one of the unique features of TRW's cell concept is that gases are generated without any apparent bubble formation or electrolyte entrainment. This is made possible by the capillary-type structure of both the electrodes and the electrolyte matrix and the use of self-regulating water feed techniques.

Prior to the work on this contract, the compact size, light weight and high efficiency of the TRW electrolysis cell had been demonstrated both on internal IR&D programs and in the 10-cell unit fabricated and operated with a carbon dioxide reduction unit under Contract NASW-650. The absence of electrolyte entrainment had been demonstrated by visual observation of the electrodes under a microscope during electrolysis (with no sign of any physical activity) and by placement of paper impregnated with phenolphthalein indicator within 0.0625 inches of the electrode surface (with no resultant discoloration during operation). The ability of the cells to achieve phase separation under actual gravity-free conditions, as well as after subjection to high launch accelerations, remained to be demonstrated.

The objective of the work on this contract was to define, design and fabricate two water electrolysis flight units, complete with instrumentation, suitable for orbital test. The purpose of the orbital test is to observe the effects of possible changes in the amount and distribution of the liquid phase in the critical regions of the cell during gravity-free operation. Due to the absence of gravitational restraints, it has been conjectured that some redistribution

of the liquid phase will occur, depending on the wetting characteristics of the different components of the cell and on the surface tension of the electrolyte. The large acceleration forces during launch could also result in some displacement or redistribution of the liquid phase. If redistribution of the liquid phase is significant, the possibility exists for gas bubbles to form in the liquid phase. Electrolyte entrainment in the effluent hydrogen and oxygen streams and a decrease in cell electrical efficiency could possibly result. Accumulation of gas-filled voids in the capillary structure could also result in interference with water transfer to the cell reaction sites, with a resultant degradation in cell performance and ultimate failure.

The scope of the contract work encompassed four major task areas - - experiment definition, instrumentation development, unit design and fabrication, and unit testing. Experiment definition encompassed selection of the optimum component configurations and operating parameters, coordination of the unit to the vehicle interfaces, and determination of the data requirements to correlate gravity-free performance with performance obtained in the laboratory. Instrumentation development was required due to the lack of any suitable conventional instrumentation for the parameters to be monitored. The work accomplished in each of these four task areas is summarized in the body of this report.

It is believed that a significant contribution was made under this contract in determination of the basic principles and parameters characterizing the projected performance of electrolysis cell units under gravity-free conditions and the effects of the various operating parameters on these characteristics. The performance attained on the units assembled on this contract verified that simple, compact lightweight electrolysis cell subsystems containing no dynamic components can be fabricated capable of extremely high performance under the ambient environmental conditions anticipated in space vehicle cabins. It remains to be verified that this performance does not degrade under launch stresses and actual gravity-free conditions.

The authors wish to acknowledge the contributions of Dr. Nicholas Fatica and Mr. John F. Reed in the experimental definition and instrumentation development phases of this program and the services of Mr. Robert P. Bajko in the design and fabrication of the instrument electronics package for the flight units.

2.0 EXPERIMENT DEFINITION

The experiment definition phase of the program consisted of a review of electrolysis cell configuration and operating parameters, as well as the other subsystem components, for potential problems under the conditions of launch acceleration and gravity-free operation. During the early months on this contract this effort was concentrated on the original wick-feed concept which was used in the CO_2 Reduction Unit fabricated under Contract NASW-650. This effort phased over to the wick-vapor-feed concept midway through for reasons which will be listed below.

The other main objective of this phase of the program was determination of the data required to correlate performance under gravity-free conditions with performance in the laboratory for the optimum component configurations and operating parameters selected above. The data required must be sufficient to pin-point the reasons for any differences which may occur as well as the magnitudes thereof.

Coordination of the flight unit configuration with the vehicle interfaces was also a part of this phase of the program. A detailed vehicle integration was not possible, however, due to lack of a specific vehicle assignment.

2.1 Wick-Feed Cell Configuration Evaluation

To evaluate the wick-feed cell for potential problems while operating in a gravity-free environment, a single cell was fabricated with transparent Lucite endplates. This cell was the same size as the one required for the flight unit (3 inch x 3 inch active electrode area). With this cell it was possible to directly observe the processes on the electrodes while the cell was in operation. The principal components of this cell, shown in cross-section in Figure 2-1, were:

a) Transparent Lucite endplates containing milled cavities for the gas spaces and water feed reservoir.

b) Nickel screen spacers for the gas cavities, which supported the electrodes and served as current collectors.

c) 100-mesh nickel screen electrodes containing a platinum/Teflon catalyst mixture.

d) A 30-mil asbestos sheet which held the KOH electrolyte between the electrodes and had a sufficiently high "bubble pressure" to permit a differ-

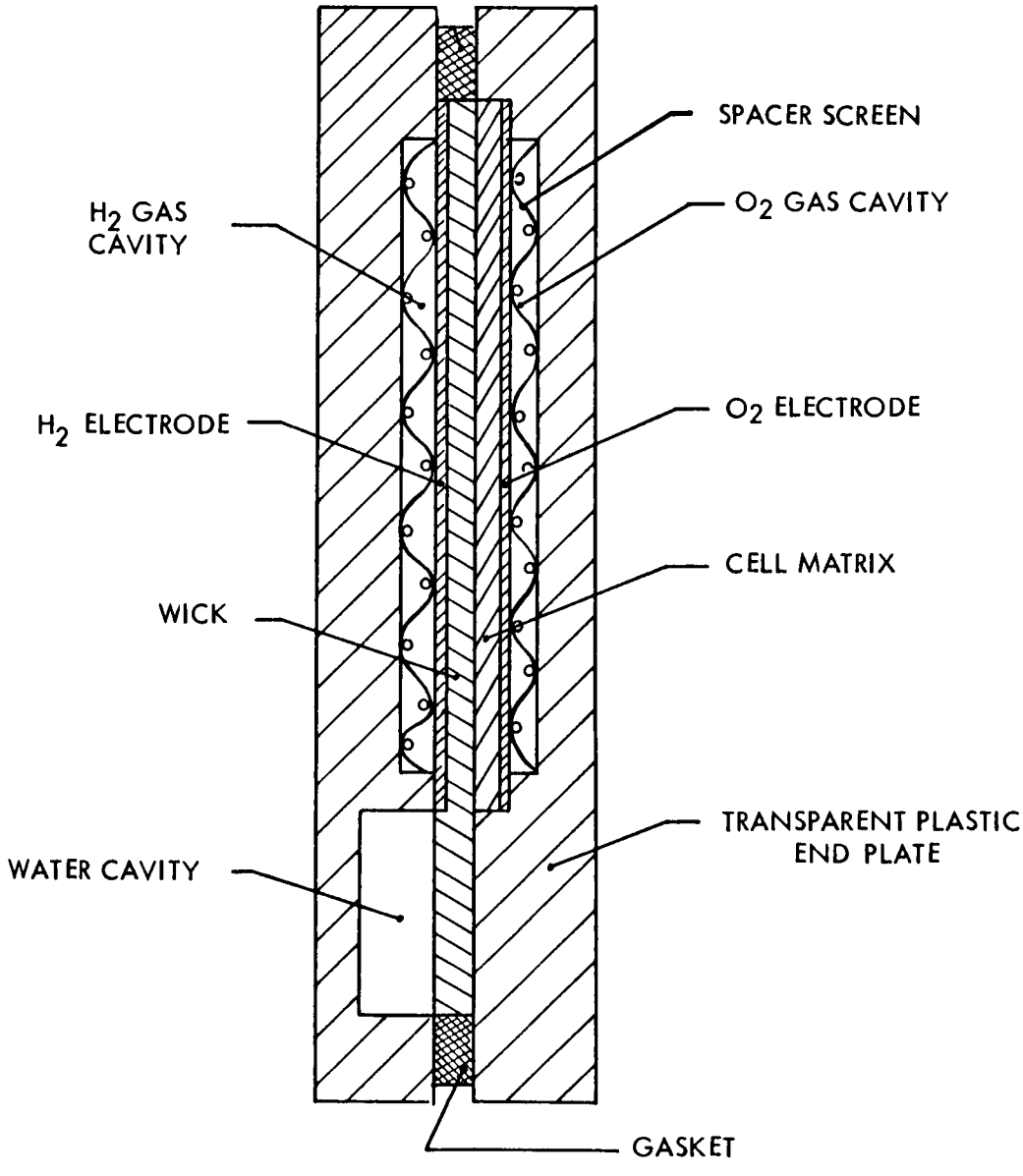

FIGURE 2-1 CROSS-SECTION OF TRANSPARENT PLASTIC CELL

ential gas pressure between the two gas compartments.

e) A polypropylene wick which extended into the water reservoir at the bottom of the cell and transported the water up to the space between the electrodes to replace water removed by electrolysis and evaporation.

Various modifications to the configuration shown in Figure 2-1 were also evaluated. These included interchanging the positions of the polypropylene wick and asbestos matrix, adding another asbestos layer to sandwich the polypropylene wick between two layers of asbestos, and varying the materials and thicknesses of the various layers.

Numerous tests were conducted with the transparent cell. The results of these tests may be classified into two categories -- physical/chemical observations of the electrode processes, and the electrical performance characteristics as a function of time. For purposes of discussion these two sets of observations are separated, although they are strongly interdependent.

2.1.1 Physical/Chemical Observations

Direct visual observations of the electrode processes led to classification of five basic effects which could pose potential problems under gravity-free operating conditions. The relationship of these effects to the various cell configurations and the interactions with electrical performance were observed.

Electrolyte Entrainment (Sputtering):

This was a transient effect, common to all configurations tested and to both electrodes. It was most pronounced immediately after initial polarization of the cell and usually subsided within one hour after initiation of testing. It was concluded that the cause of this effect was the level of electrode saturation existing after initial vacuum-charging of the cell with electrolyte. Since gas evolution is not localized to a gas-liquid interface, excess liquid bridging the electrode reaction sites could be expected to be displaced by the evolved gases at higher current densities.

To verify this theory, a small open cell was fabricated wherein the electrodes could be observed directly under a microscope while in operation without any intervening media. Electrolyte was added to the cell with an eye-dropper to

observe the effect of the amount of electrolyte in the cell matrix on gas bubble formation. When electrolyte loading was such that the electrode surface glistened, or appeared wet, surface activity was observed which could result in sputtering. However, when electrolyte loading was such that there was no liquid sheen on the electrode surfaces, no sign of surface activity or sputtering was evident at current densities up to 100 amperes per square foot. It was thus concluded that, with proper control over the water feed system, it should be possible to prevent sputtering as a source of electrolyte entrainment in the effluent gas streams.

Solute Crystallization:

This effect was observed on all configurations tested, but was confined to the cathode (hydrogen electrode). The crystallization was observed with both pure water feed systems and aqueous KOH feed. The general pattern of crystalline growth observed was from the geometrical center of the electrode outward towards the edges. The amount of crystallization was a function of continuous time under load. In several instances the expansion of a crystal would displace the platinum particles from the substrate nickel screen resulting in loss of electrode catalyst.

The cause of this crystallization was probably a combination of factors:

a) An unbalance in the water consumed by the reaction and that transported to the reaction sites via the wick (i.e., insufficient wicking rate), and
b) The wick does not selectively transport water to the reaction sites (i.e., for a given volume of water consumed the wick will transport an equivalent volume of aqueous KOH.

As a result of these factors a point was reached where the localized concentrations of KOH in certain areas of the cathode exceeded the solubility limit.

In partial verification of the above theory, an operational cell which had developed a gross amount of crystallization was allowed to stand at open circuit conditions for 14 hours. Following this period the following observations were made:

a) The cell had wicked additional water from the feed reservoir.
b) The crystals had dissolved.

c) Particles of platinum black, torn from the electrode, were found in the mesh of the supporting screen.

It was obvious that the required water balance in the cell had not been satisfied during operation under load.

Electro-Osmotic Transport:

A net continuous transport of liquid to the cathode gas cavity was observed in several cell configurations. There appeared to be a maximum height to which the liquid could rise and be sustained in the cathode cavity (approximately one inch over the bottom of the electrode). It was subsequently demonstrated that running the cell with a slightly elevated pressure in the gas cavities was sufficient to prevent liquid accumulation. (It was also shown that reversal of polarity would result in reversal of the direction of liquid transport.)

Foaming :

Foaming was observed during the startup period in a number of tests wherein the wick was adjacent to one of the electrodes. This appeared to be a transient effect associated with fresh solutions of KOH. The severity of foaming also appeared to be dependent upon which electrode was adjacent to the wick, the most foaming occurring with the oxygen electrode immediately adjacent to the wick. Since this phenomenon was associated with fresh solutions of KOH, it was probably the result of surfactant action of trace impurities. Pre-aging, or possibly pre-electrolyzing, the electrolyte would probably eliminate this problem.

Liquid Displacement:

Simple spin tests on various simulated cell matrix configurations indicated that problems would be encountered under high launch accelerations with the polypropylene wick material adjacent to one of the electrodes. However, no runoff or displacement of liquid from the matrix was observed at accelerations up to 15 g's when the wick material was sandwiched between two layers of asbestos. This arrangement was utilized in the later cell tests with the wick-feed concept, even though a thicker matrix, and hence a somewhat higher internal cell resistance, resulted.

2.1.2 Electrical Performance Characteristics

An excessive rate of cell polarization was obtained on all early tests with the transparent test cell. Typical voltage-time characteristics obtained for several cell configurations are shown in Figure 2-2. A rapid increase in cell terminal voltage was observed on all cells within the first several hours, with the voltage increasing to 2.0 to 2.1 volts within 24 hours. (Cell current was held constant at 100 amperes per square foot in all runs.) One cell using an asbestos wick instead of the polypropylene wick had a terminal voltage increase to 2.2 volts within 8 hours. Tests were conducted using both pure water feed to the cells and 30% (by weight) KOH, with no significant difference over a 24 hour period. All tests were initiated at ambient laboratory temperature, with the internal cell temperature rising to approximately 105°F to 115°F after a few hours.

Visual observations during the above tests verified that a wicking rate limitation was present, with solute crystallization ultimately occurring in all cases. It was postulated that this limitation was caused by excessive compression of the wick in the land area forming the gas seal between the gas cavities and the water feed reservoir.

To allow closer control over the compression of the feed wick, two additional experimental cells were fabricated. One cell was of all metal construction, while the second was a composite structure of metal and plastic. Both cells had a machined pin structure in the gas cavities to replace the spacer screens used in the transparent plastic cell. A photograph of the composite experimental cell components is shown in Figure 2-3.

The composite metal/plastic cell was fabricated after it was found that the voltage rise with time using the metallic cell was even more rapid than in the plastic cell. It was postulated that electrolysis was occurring in the wick in the land-seal area of the metallic cell, forming captive gas bubbles in the wick and restricting water feed to the cell.

Improved performance was obtained on the composite cell. However, it was subsequently observed that equivalent performance could be obtained with the original

CELL TYPE: TRANSPARENT TEST CELL
ELECTROLYTE: 30% (BY WEIGHT) KOH
ELECTRODE TYPE: AMER. CYAN. TYPE AB-1
CURRENT DENSITY: 100 ASF (6.25 AMPS)
TEMPERATURE: AMBIENT (INITIAL)

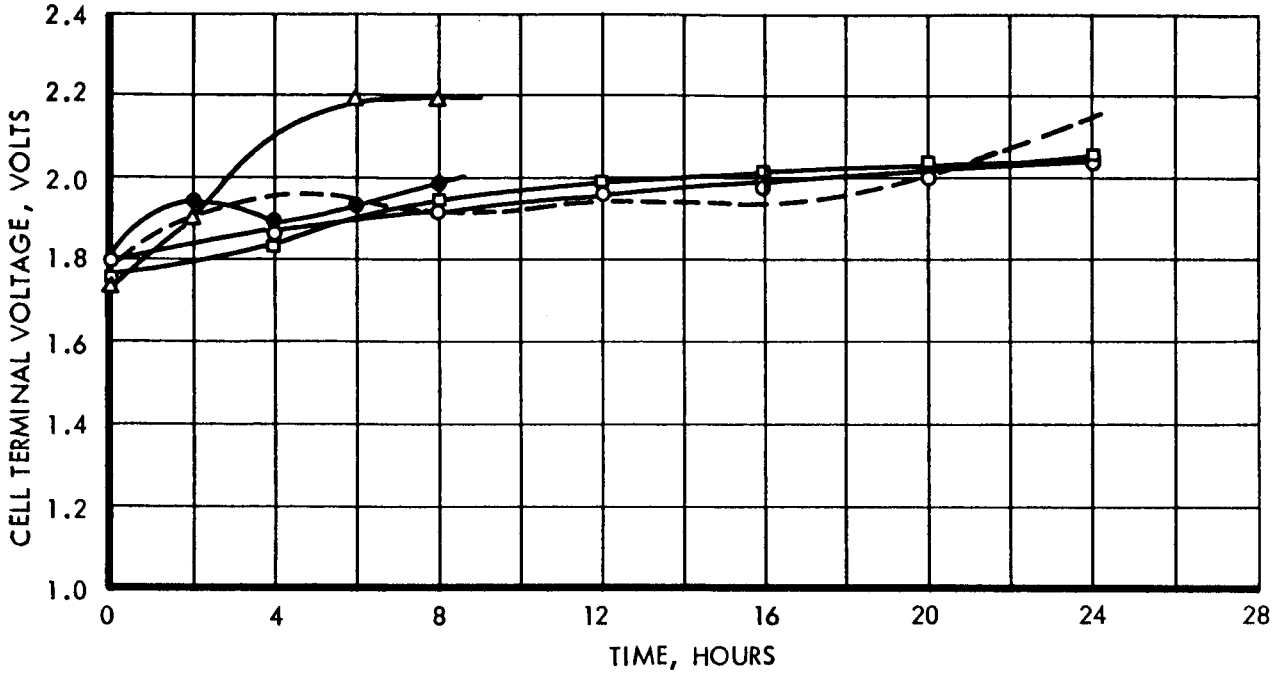

CONFIGURATION*	INITIAL RESERVOIR SOLUTION	TERMINAL CELL TEMPERATURE (°F)
o H/PW/A/O	30 WT % KOH	113
□ H/A/PW/O	30 WT % KOH	113
△ H/AW/A/O	H_2O	113
--- H/A/PW/A/O	H_2O	108
● H/A/PW/O	H_2O	108

*THE SCHEMATIC CONFIGURATION H/PW/A/O IS INTERPRETED AS FOLLOWS: POLYPROPYLENE WICK ADJACENT TO THE HYDROGEN ELECTRODE. ASBESTOS GAS BARRIER ADJACENT TO THE OXYGEN ELECTRODE.

FIGURE 2-2 VOLTAGE - TIME CHARACTERISTICS FOR VARIOUS CELL CONFIGURATIONS

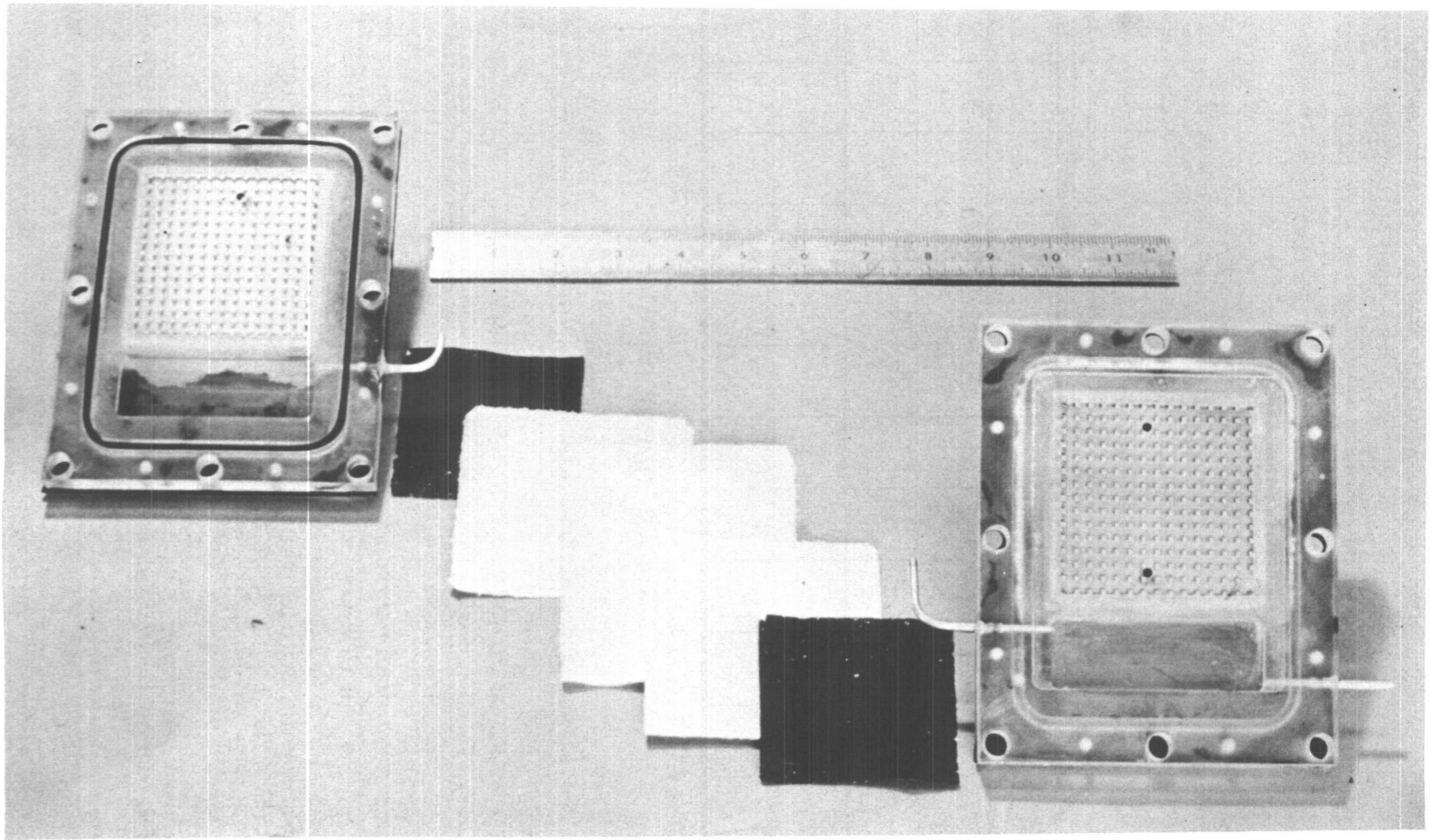

FIGURE 2-3 COMPOSITE METAL/PLASTIC EXPERIMENTAL CELL

transparent cell by using a plastic spacer between the endplates to control compression on the wick. Figure 2-4 shows two typical runs subsequently obtained on the plastic cell while holding the compression on the wick in the land-seal area to approximately 0.032 inches. (Uncompressed thickness of the wick is approximately 0.050 inches.)

Further attempts to improve performance on the wick-feed cells were concentrated on elimination of possible oxide films on the anode side of the cell. In earlier tests a tarnish-like film had been observed on the nickel anode current collector screens. Elimination of bare nickel surfaces on the anode side, by gold plating the anode current collector screen and using electrodes with a gold plated substrate screen, resulted in much improved performance. Two typical runs obtained using the gold plated hardware are shown in Figure 2-5. Both the rate and level of polarization were significantly lower than observed in the earlier tests.

Curve (2) in Figure 2-5 was conducted with a back pressure of 6 inches of water on both gas cavities. During this test no free liquid was observed in either gas cavity. This test served as verification that the accumulation of liquid due to the electro-osmotic transport phenomena could be avoided as discussed previously.

2.2 Selection of Wick-Vapor-Feed Cell Configuration

TRW in-house investigations of advanced types of water electrolysis subsystems for space vehicle atmosphere control proceeded in parallel with the work on wick-feed cells under this contract. During this period high performance was demonstrated on two advanced types of cells, the vapor-feed and wick-vapor-feed concepts. The in-house work on the wick-vapor-feed concept had a direct influence on the present contract.

As originally conceived, the wick-vapor-feed concept utilized a feed wick to transport water from an external reservoir to each cell. The wick was, in effect, distributed over the back of the hydrogen cavity in each cell. A perforated, nonporous sheet and a feed matrix were placed over the feed wick in each cell. The hydrogen gas cavity in each cell was formed by a spacer screen between the feed matrix and the hydrogen electrode. The cell itself consisted of two

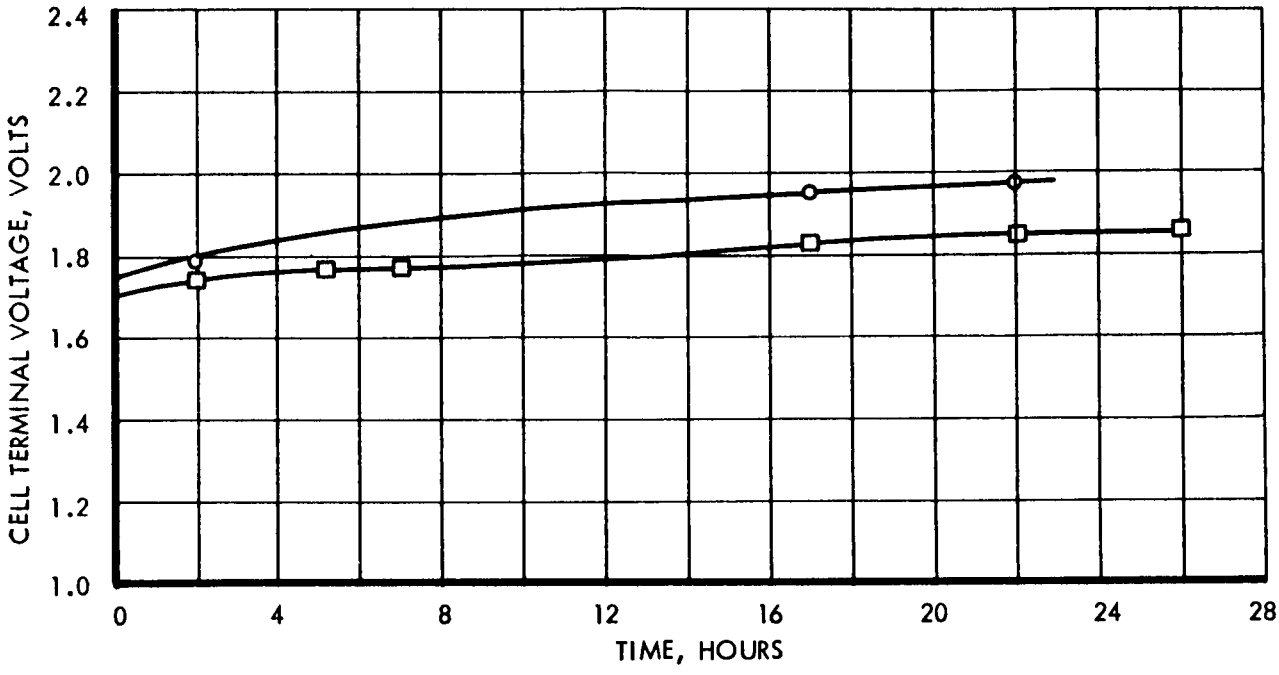

CELL TYPE: TRANSPARENT TEST CELL (PLASTIC SPACER)
ELECTROLYTE: 32% (BY WEIGHT) KOH
ELECTRODE TYPE: AMER. CYAN. TYPE AB-1
CURRENT DENSITY: 100 ASF (6.25 AMPS)
TEMPERATURE: AMBIENT (INITIAL), 93°F (TERMINAL)
CONFIGURATION: H/A/PW/A/O

FIGURE 2-4 VOLTAGE - TIME CHARACTERISTICS WITH CONTROLLED WICK COMPRESSION

CELL TYPE: TRANSPARENT TEST CELL (PLASTIC SPACER)
ELECTROLYTE: 32% (BY WEIGHT) KOH
ELECTRODE TYPE: AMER. CYAN. TYPE AB-6
CURRENT DENSITY: 100 ASF (6.25 AMPS)
TEMPERATURE: AMBIENT (INITIAL)
CONFIGURATION: H/A/PW/A/O

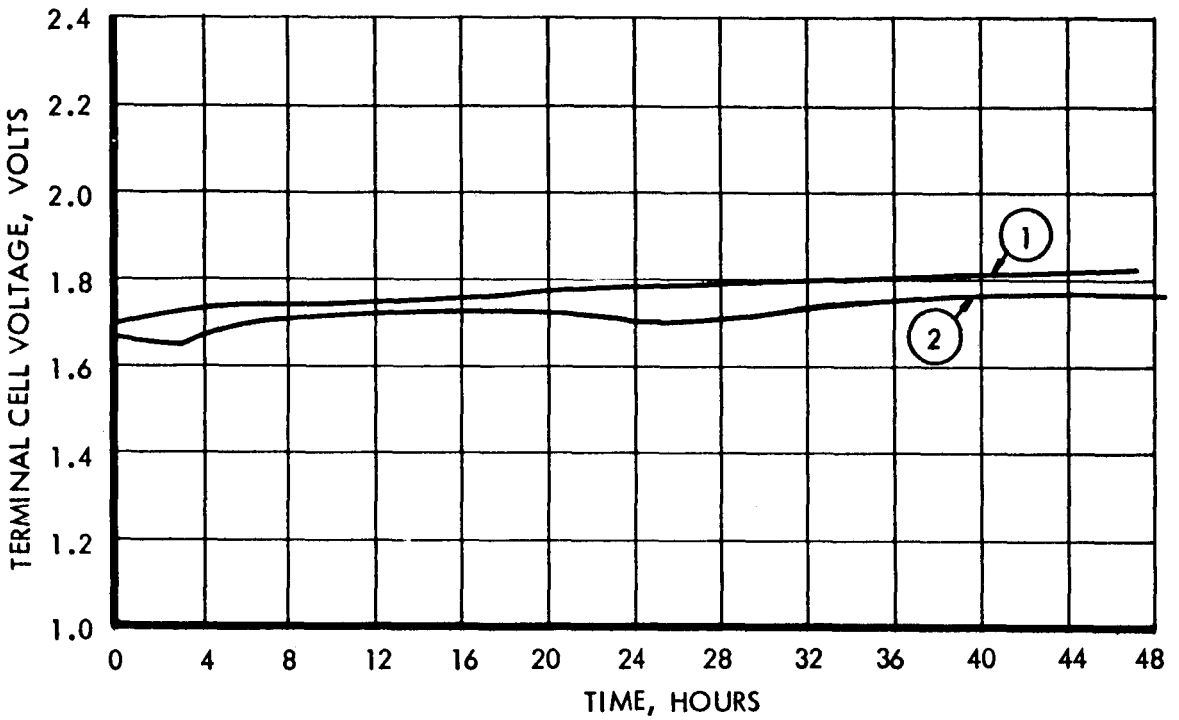

NOTE:

(1.) HYDROGEN ELECTRODE: TYPE AB-1. SAME ELECTRODE USED IN TESTS SHOWN IN FIGURE 2-4.

(2.) HYDROGEN GAS PRESSURE = OXYGEN GAS PRESSURE = 6 INCHES H_2O WATER CAVITY PRESSURE = AMBIENT.

FIGURE 2-5 VOLTAGE - TIME CHARACTERISTICS FOR GOLD PLATED ANODES

screen electrodes sandwiching an asbestos electrolyte matrix. The cell matrices and feed matrices were to be charged with the same concentration electrolyte, while the feed wicks were to be charged with water.

In operation, water would be consumed at the hydrogen electrode in accordance with the half-cell reaction

$$2\ H_2O + 2\ e^- \longrightarrow 2\ OH^- + H_2\uparrow$$

thus increasing the concentration of the catholyte. Water vapor would flow from the feed matrix to the cell matrix under this concentration difference at a rate proportional to demand. As water was evaporated from the feed matrix, it would be replenished by the wick system. The perforated sheet would serve to provide a convectional velocity through the perforations greater than the diffusional rate of electrolyte in the reverse direction, thus minimizing feed matrix concentration reduction by back diffusion into the water feed wick.

The above mode of operation would provide water feed to the entire face of the cell, thereby avoiding the lateral concentration gradients inherent in edge-fed cells. Other advantages would include the capability to feed water at low pressure to a cell operating at higher gas pressures and removal of the wick from between the electrodes, permitting higher cell performance while retaining a static feed system.

In test cells employing the wick-vapor-feed concept, it was found that both the feed wicks and the perforated sheets could be eliminated. A schematic representation of an experimental nickel-plated test cell is shown in Figure 2-6. With this configuration it was possible to assemble the unit dry and subsequently vacuum charge the entire unit with the same concentration electrolyte. The electrolyte was then expelled from the oxygen cavity by gas pressurization and then from the hydrogen cavity by application of a somewhat lower pressure. Maintainance of the oxygen cavity pressure higher than the hydrogen cavity pressure, which in turn was held higher than the feed cavity pressure, assured that any free electrolyte in either gas cavity would be rejected to the feed cavity. In operation, makeup water was supplied to the feed cavity from an external reservoir, while the proper pressure gradients were maintained by control of gas back pressures.

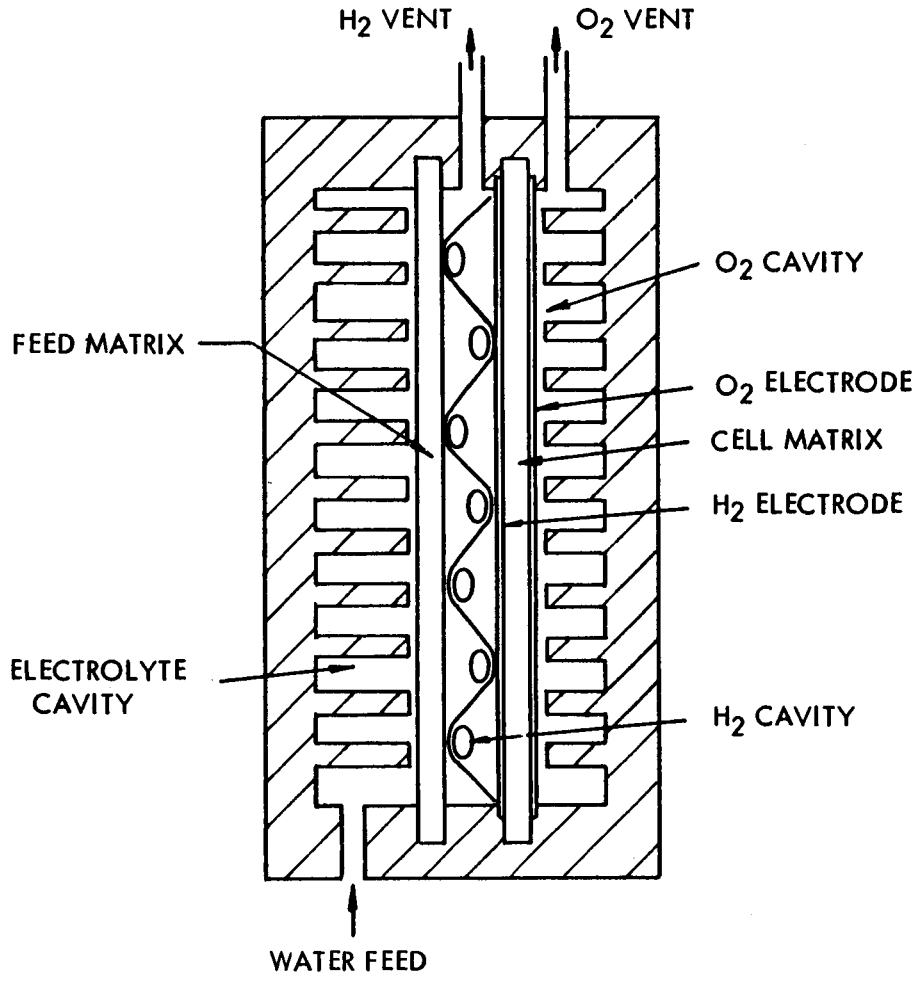

FIGURE 2-6 SCHEMATIC CROSS-SECTION OF WICK VAPOR FEED CELL

A 73-hour exploratory test run on the experimental wick-vapor-feed cell is shown in Figure 2-7. The cell was operated in both the vertical and horizontal positions (with the liquid feed cavity on top) with no evidence of liquid in either of the transparent gas discharge lines. This verified that the liquid phases within the cell were maintained in place by the capillary potentials of the respective matrices. The back pressure regulators were re-adjusted several times during the run to demonstrate insensitivity to pressure or pressure differential once the gas cavities were cleared of electrolyte.

At 69 hours of operation (Figure 2-7) gas was vented from the feed cavity of the cell with an immediate appreciable decrease in cell voltage. Subsequent tests disclosed that the feed cavity could accumulate appreciable amounts of gas, displacing so much of the liquid in the cavity that the feed matrix would dry. The problem was traced to the presence of dissolved gases in the feed water which could be eliminated by vacuum boiling the feed water in the external reservoir prior to connection to the cell.

The small continuous rise in cell voltage with time was attributed to the formation of nickel oxide on either (or both) the nickel substrate screen in the anode or the nickel-plated endplates. Other tests with gold-plated electrode screens and gold-plated endplates showed virtually no increase in cell voltage with time. (See Figure 2-8.)

At this point in the program, by mutual agreement between TRW and NASA, based on the data generated under TRW's in-house program, the wick-vapor-feed configuration was selected for use in the flight unit. This conclusion was based on the following reasons:

a) A higher cell voltage efficiency was attainable on the wick-vapor-feed cell.
b) Scaleup in cell size should be no problem for this configuration, while it may pose problems for the wick-feed configuration.
c) Internal gas sealing is much easier in the wick-vapor-feed configuration, allowing much larger differential gas pressure tolerances.
d) The wick-vapor-feed configuration will withstand higher launch accelerations without displacement of free electrolyte into the gas cavities.

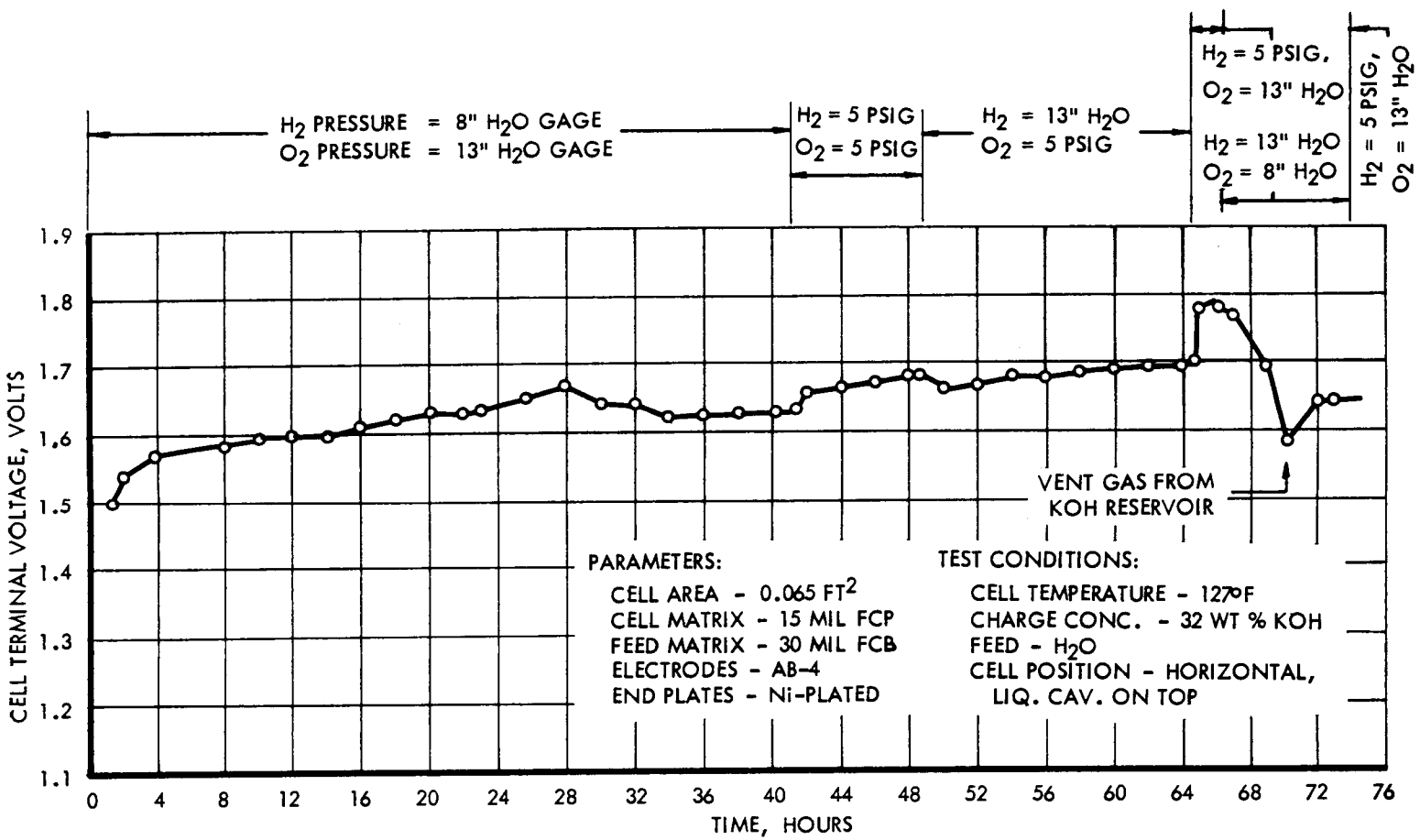

FIGURE 2-7 EXPLORATORY TEST ON EXPERIMENTAL WICK-VAPOR-FEED CELL

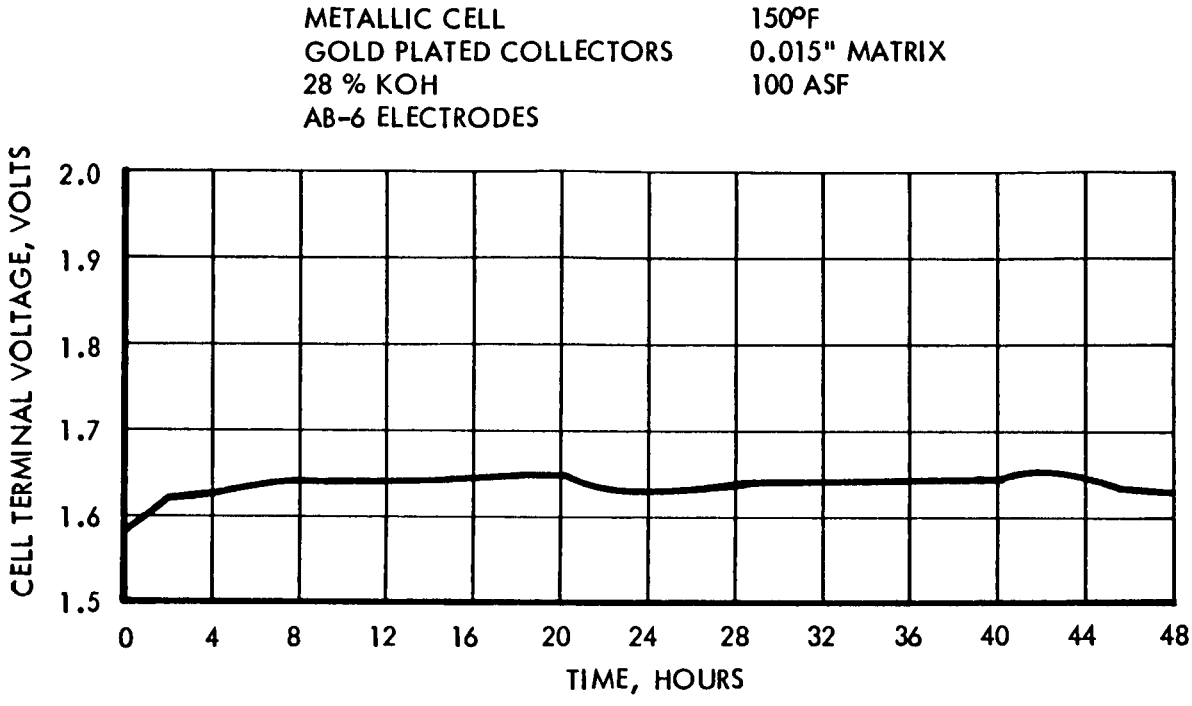

FIGURE 2-8 EXPERIMENTAL TEST ON GOLD PLATED CELL HARDWARE

e) The likelihood of electrolyte entrainment in the effluent gases is potentially less for the wick-vapor-feed cell.

f) Long term voltage degradation appears to be negligible in the wick-vapor-feed configuration, while erratic performance with time has been obtained on wick-feed cells.

No further work was done on the wick-feed configuration under this contract. All subsequent work involved the wick-vapor-feed configuration.

2.3 Determination of Operating Parameters and Data Requirements

To establish the relationship between cell voltage and temperature (at a current density of 100 ASF) runs were made at five different temperatures. The interpretation of these data was complicated by the fact that there was a continuous increase of cell voltage with time as the test series was run. (Gold-plated hardware was not used.) Nevertheless, a 20 hour run at 122°F and another at 156°F disclosed that the voltage increase with time was constant at both temperatures; therefore all the plots of voltage versus time were extrapolated to a common time. The resulting voltage-temperature relationship is shown in Figure 2-9 for nickel-plated end plates and nickel screen electrodes.

A typical voltage-current characteristic is shown in Figure 2-10. This polarization curve was taken approximately 50 hours after start of testing, at a temperature of 155°F.

The above observations were reviewed along with the contract Statement of Work. This review resulted in selection of the design operating parameters shown in Table 2-1.

The design current density was established in the contractual agreement.

The cell stack temperature selected was the maximum permitted in the contractual agreement to provide minimum cell voltage and hence minimum power on the flight vehicle. Selection of this temperature also results in a conservative design from the standpoint of materials selection as well as calculation of the maximum water reservoir capacity which may be required in the flight unit.

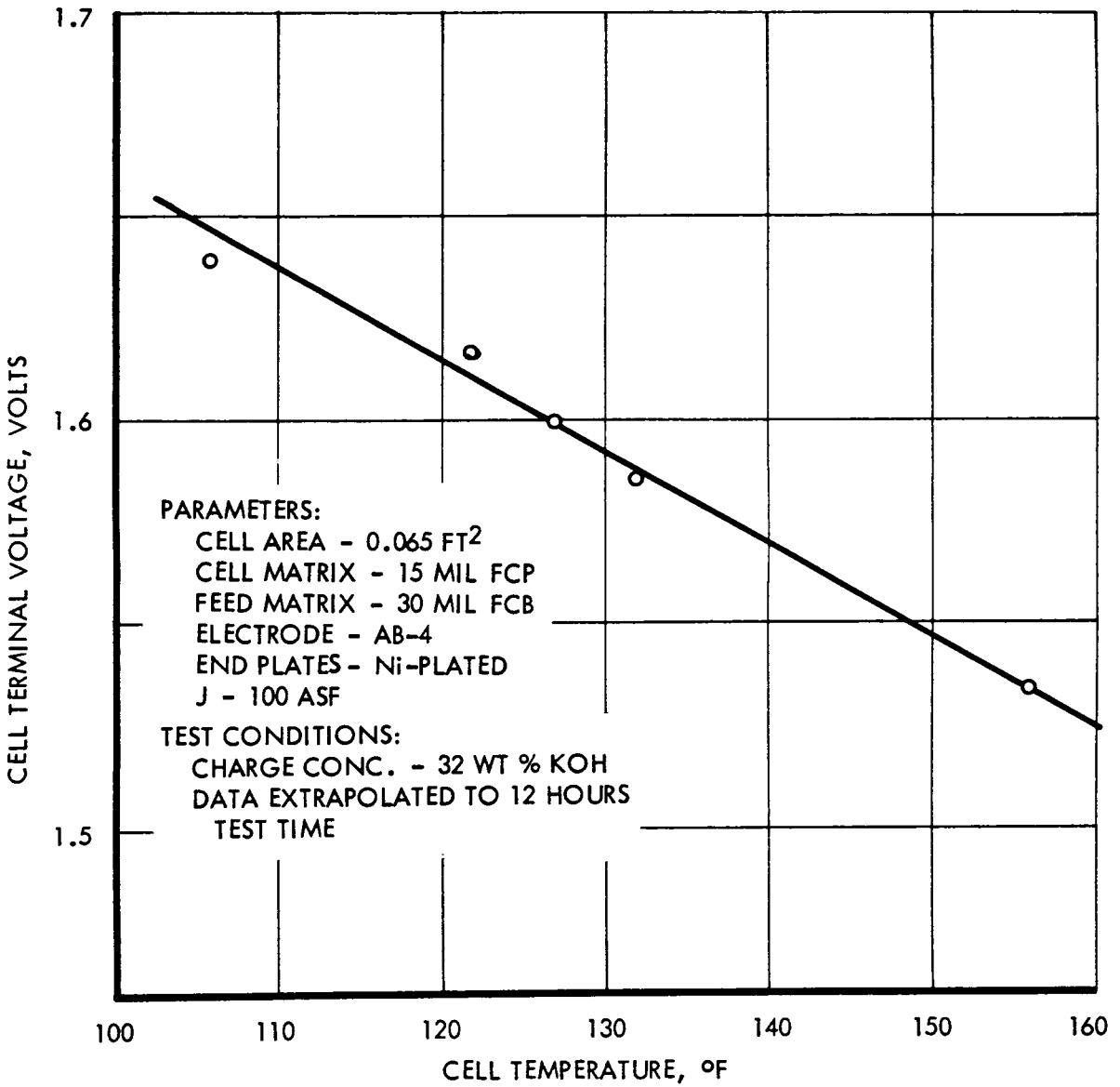

FIGURE 2-9 VOLTAGE - TEMPERATURE CHARACTERISTICS FOR WICK-VAPOR-FEED CELL

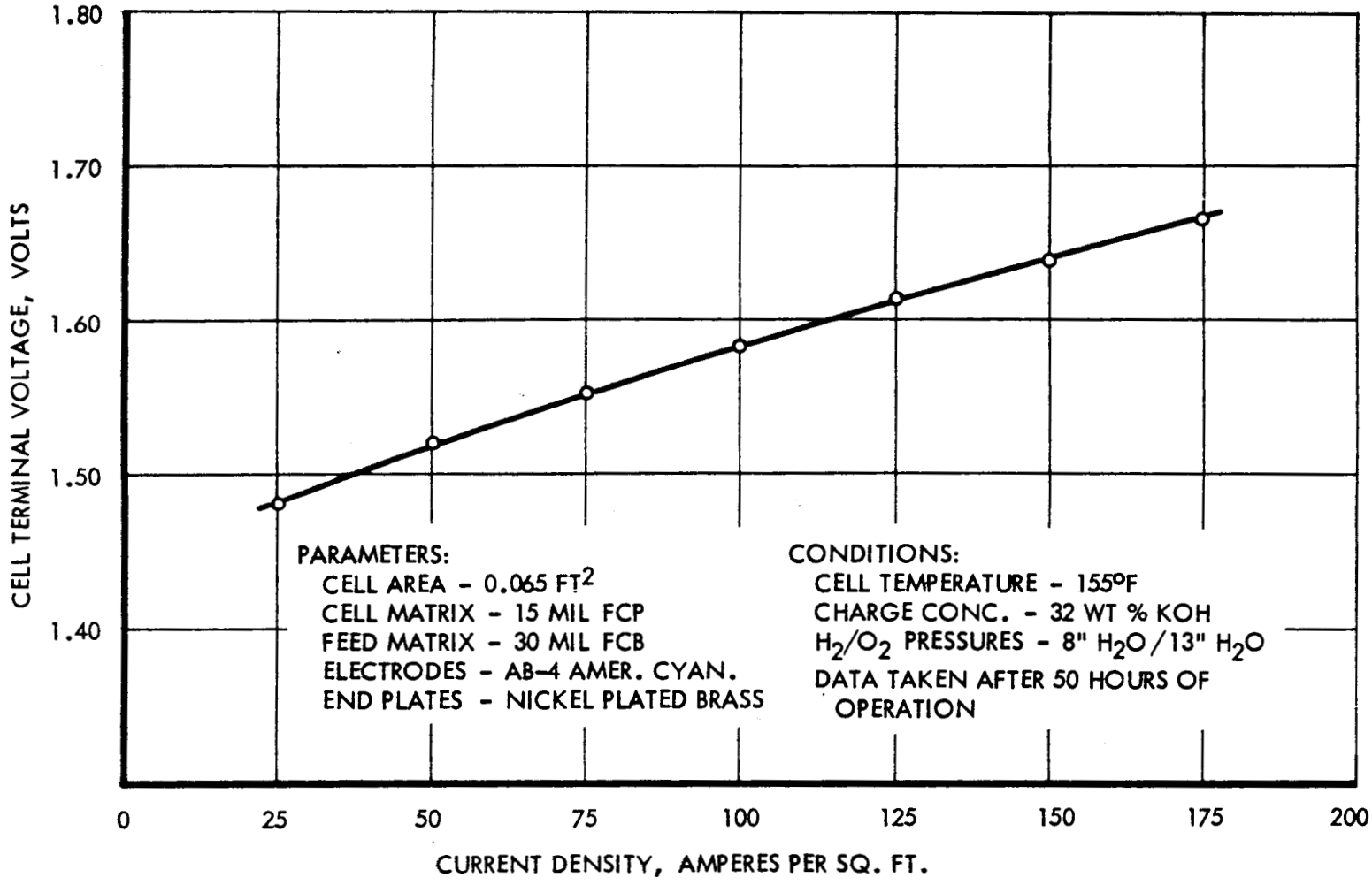

FIGURE 2-10 TYPICAL POLARIZATION CURVE, WICK-VAPOR-FEED CELL

TABLE 2-1

Design Point Operating Parameters

Cell Current Density	100 Amperes/Square Foot
Cell Stack Temperature	140°F
Electrolyte Concentration	32% KOH (By weight)
Oxygen Cavity Pressure	15.7 psia
Hydrogen Cavity Pressure	14.7 psia
Feed Water Pressure	13.7 psia (Reservoir Full)
	11.4 psia (Reservoir Empty)
Duration of Flight Operation	24 hours

Electrolyte concentration was specified to provide maximum specific conductance and hence minimum ohmic polarization. Performance obtained on experimental cells has shown very little sensitivity to electrolyte concentration over a wide range above and below this value.

The pressures were selected at a nominal value of one atmosphere with the highest pressure on the oxygen side and the lowest in the electrolyte cavity. This arrangement assures that any free electrolyte will be rejected to the electrolyte cavity. The bubble pressures for the 15-mil and 30-mil asbestos were specified as 23 psid and 52 psid respectively; consequently the design pressure differentials are well within tolerable limits. The major pressure requirement is to assure that the electrolyte cavity pressure is always below the hydrogen cavity pressure to prevent flooding of the hydrogen cavity.

Duration of flight operation must be sufficient to demonstrate effects of a gravity-free environment, yet as short as possible to minimize power requirements and package weight (i.e., water supply system weight). Both analytical computations and experience on experimental cells indicate that equilibrium performance should be reached within approximately 8 hours. The 24 hour duration should therefore be sufficient to observe effects of gravity-free operation on the phase separation characteristics of the electrolysis unit.

The data requirements selected for the flight unit are tabulated in Table 2-2. With this data it is intended to monitor the mass and energy balances around the cells as well as to analyze any malfunctions or discrepancies between gravity-free and laboratory performances which may occur.

Gas pressure data used with the precalibrated capillary tubes will provide a measurement of gas evolution rates. Measured gas evolution rates can be correlated with the rates deduced from current consumption to determine whether there is external, or internal, gas leakage. Internal leakage would also be indicated by a partial or complete reduction of pressure differential between the two gas cavities. The resultant internal gas mixing would also be indicated by the contaminant sensor in the hydrogen side analytical train as well as by the stack temperature sensor.

TABLE 2-2

Flight Unit Data Requirements

Absolute Pressure of Oxygen Cavities
Absolute Pressure of Hydrogen Cavities
Absolute Pressure of Water Feed System
Cell Stack Temperature
Cell Current
Cell Voltages (3)
Effluent Hydrogen Temperature
Effluent Oxygen Temperature
Effluent Hydrogen Humidity
Effluent Oxygen Humidity
Hydrogen Contamination of Effluent Oxygen
Oxygen Contamination of Effluent Hydrogen
Electrolyte Entrainment in Effluent Hydrogen (2)
Electrolyte Entrainment in Effluent Oxygen (2)

Liquid pressure data along with a prior calibration of the water reservoir will provide a measurement of water consumption. A leak through the feed matrix would allow hydrogen to enter the reservoir and would result in a reduction of the pressure differential between the hydrogen gas and the liquid. Inter-cell electrolysis would result in a build-up of gas inventory within the feed cavities and an increase in liquid pressure.

Stack temperature is obviously a variable of primary significance. (See Figure 2-9.) Due to the relatively high thermal conductance of the cell stack materials, a single temperature sensor will provide a measure of mean stack temperature. Rapidly increasing temperature could indicate internal gas leakage and combustion, while a drop in temperature could indicate an external liquid leak with resultant cooling of the stack by water evaporation.

Stack current is a primary variable and of necessity must be monitored. A breakdown in the dielectric film between adjacent cells would be indicated by excessive total current; a reduction of current could be indicative of an increase in cell resistance as the result of cell drying.

The voltage (at a constant current density) has been found to be the primary indicator of cell performance, and hence the voltage of each cell will be monitored individually. An increase in cell voltage could be caused by an increase in activation, concentration or ohmic polarization. These are complex functions of operating conditions, but the most common reason for voltage increase is an increase in ohmic polarization as the result of cell drying or the formation of metallic oxide films. Loss of catalytic activity and concentration polarization are usually not significant factors except in the case wherein cell drying occurs which subsequently results in the loss of catalytic sites and excessive current densities at the remaining sites.

Measurement of relative humidity, temperature, pressure and entrainment in each of the effluent gas streams, along with the cell stack parameters already discussed, will allow mass and energy balances around the cells to be calculated. Other parameters such as the water vapor losses in the effluent gas streams, changes in mean cell electrolyte concentration and the mass of any entrained KOH in the gas streams will be calculated from these parameters. For example, the

partial pressure of water vapor existing in equilibrium above the electrolyte is a function of the solution concentration and temperature. Therefore, measurement of relative humidity and temperature provides an indication of electrolyte concentration. Correspondingly, a change in electrolyte concentration would cause a variation in humidification of the effluent gas streams, a change in mass flow through the capillary tubes, and hence a change in the gas pressure readings.

The conductivities of the electrolyte entrainment sensors in the effluent gas streams are affected by the water vapor partial pressures in the respective gas streams. The entrainment calibrations must therefore be defined as functions of the gas temperatures and relative humidities. Two entrainment sensors are located in series in each gas stream so that a differential measurement, theoretically independent of temperature and humidity effects, can also be obtained to verify whether or not entrainment is occurring. Use of two stages in series also helps ensure that no entrainment reaches the gas instrumentation transducers in the down stream analytical trains.

2.4 Coordination of Experiment to Vehicle Interfaces

Since a vehicle assignment or definite selection of type of launch vehicle has not yet been made, unit design did not encompass vehicle integration considerations in conformance to a specific set of environmental and geometrical specifications.

However, at the recommendation of the Technical Monitor, discussions were held with representatives of Spacecraft, Inc. (Huntsville, Alabama) relative to possible integration into their "01" Standard Payload Module (SPM). It was mutually agreed that integration of the TRW Electrolysis Unit for Orbital Test into the SPM was feasible. The largest question was whether the SPM will be capable of providing a reasonable environment for time periods approaching 24 hours in duration.

For the specific unit design it was assumed that the unit will be mounted in a package similar in configuration to the SPM. Specifically, the unit was designed to mount to a flat, rigid mounting plate which is maintained at a temperature of

70°F. The effluent hydrogen and oxygen gases will be vented to the ambient environment which was assumed to be unpressurized (space vacuum). An external source of dc power will be provided for the Electrolysis Unit and an external telemetry package and/or data recording system will be provided to transmit the dc voltage signals received from the Electrolysis Unit back to Earth. Startup of the unit will be accomplished in orbit.

3.0 INSTRUMENTATION DEVELOPMENT

Conventional components were selected and/or modified to measure temperatures, pressures, current and humidities. However, it was necessary to develop instrumentation to measure electrolyte entrainment and contamination (mixing) in the effluent gas streams. The capillary flow tubes for gas flow rate measurement and control of gas back pressures were also fabricated at TRW, as were the instrumentation electronics packages which contain circuits to provide power to all the transducer elements and to condition all the signal outputs to the vehicle telemetry system.

3.1 Selection of Conventional Instrumentation

3.1.1 Temperature Sensors

Both the gas temperature and the gas contamination sensors use a thermistor element supplied by Fenwal Electronics Inc. "Iso-curve" thermistors were selected, and are so called because they have a characteristic matched to a standardized resistance-temperature curve published by the manufacturer.

The specifications certified by the manufacturer were as follows:

Type: GB32JM22 Iso-curve matched $\pm$ 1°F in the range 60°F to 150°F
Resistance at 77°F: 2000 ohms
Thermistor will perform satisfactorily after being subjected to the following vibration levels:

a) 0.5 inches double amplitude at 5 to 14 cps (sinusoidal)
b) 5 G zero-to-peak acceleration at 14 to 400 cps (sinusoidal)
c) 10 G zero-to-peak acceleration at 400-3000 cps (sinusoidal)

The small size of the bead thermistor was also compatible with design of an analytical train housing no larger than 0.5 inches diameter.

3.1.2 Pressure Transducers

The Statham, miniature, flush diaphragm, unbonded strain gage, pressure transducer, PA 208 TC -25- 350 was selected for all pressures. The specified range was 0 to 25 psia with 200% overload capacity. The transducers were supplied with stainless steel port material for compatibility with the

electrolyte. With 5 volt excitation, the output voltage at a minimum pressure of 11.4 psia is 18 millivolts.

The supplier certified that the units would be capable of satisfactory performance to specified accuracies after being subjected to the following launch conditions:

a) Shock: 30 G peak for 8 milliseconds
b) Vibration:
   i) 0.5 inches double amplitude at 5 to 14 cps (sinusoidal)
   ii) 5.0 G zero-to-peak acceleration at 14 to 400 cps (sinusoidal)
   iii) 7.5 zero-to-peak acceleration at 400 to 3000 cps (sinusoidal)
c) Acceleration: 15 G for 90 second duration

These specifications were predicated on orbital start-up.

Alternative units were considered and discarded on the basis that their performance, size, weight or cost did not meet the requirements of the package. Major requirements were size (the unit had to be mounted on the analytical train), availability and cost.

3.1.3 Current Sensors

Stack current was measured by means of a Janco, 50 millivolt, DC current shunt rated at 10 amperes (Specification MIL-S-61B). The standard accuracy of the unit is 0.5%. At the design current density of 100 amperes per square foot, the stack current is 6.25 amperes, corresponding to an output of 31.25 millivolts. This unit has been utilized in the Gemini vehicle and was selected on this basis.

3.1.4 Humidity Sensors

Most of the existing methods for detecting and indicating humidity were not suitable for the orbital experiment. A generalized grouping of available devices and the reasons which eliminated their incorporation are summarized in Table 3-1. This brief survey suggested that an electric hygrometer of the conducting-film type was the most logical choice to meet the conditions imposed by the experimental geometry. The Phys-Chemical Research Corporation sensor,

TABLE 3-1

Survey of Methods for Humidity Measurement

Device	Disadvantages
Mechanical hygrometers	Susceptible to damage in launch environment; requires additional transducer to bring signal to electronic interface.
Gravimetric methods	Will not function in gravity-free space.
Psychrometer	Requires a water supply to instrument.
Condensing hygrometer	Requires the flow of a refrigerant, an optical system with a light source and a thermal control system.
Measurement of infrared absorption	Highly complex and costly.
Index of refraction or magneto-optical rotation	Effects would be too small in the geometry of the experiment to warrant consideration.
Neutron thermalization:	Neutron source highly undesirable complication of the experiment.

Type PCRC-55, was selected because of its small size and its response over the full humidity range from 0% to 100% RH. The sensor is a plastic wafer composed of a conducting film coated on a styrene substrate. Changes in relative humidity cause the surface resistivity to vary. Only a small modification to the terminals was necessary to allow the standard sensor to fit inside the 0.5 inch diameter analytical train housing.

3.2 Electrolyte Entrainment Sensors

No commercially available sensor was found which could be adapted to detect an aerosol dispersion of KOH within the geometry of the experiment. Development of a sensor was accomplished semi-empirically after a theoretical study of general methods of detecting the entrainment.

Three groups of techniques were considered:

a) Accumulative separation of KOH from the gas stream.
b) Detection of KOH without disturbing the aerosol.
c) Sampling some fraction of the flow.

Instruments classified in Group b were found too complex and costly. Methods considered included:

a) Ionization effects involving K^+ ions
b) Light scatter measurements
c) Atomic absorption spectrophotometry.

Sampling techniques were rejected because instrumentation downstream (for example the humidity sensor) would be adversely affected by residual entrainment. It was decided therefore that the sensor function should be based on an effect attributable to the total mass of the entrained KOH.

The final choice was made between two devices. The first device filtered KOH from the stream with a matrix held between electrically conducting screens. A small cell was formed in which the conductivity would vary as a function of the mass of KOH in the filter.

The second device allowed the entrained KOH to etch a coating of aluminum vapor-deposited on a mylar film. In the places where KOH and aluminum reacted, the mylar would transmit light to a photoresistive element. This method was discarded because the thickness of the aluminum film on commercially available coated mylar varied over too wide a range for the method to be considered quantitative. In addition, a light source and its power supply would be required, while the simplier conductivity sensor would not require any auxiliary apparatus.

An experimental model of the conductivity cell entrainment sensor was constructed from a 0.4 inch diameter disc of Dynel M1450 fabric held between platinum screens. A stream of oxygen containing entrained KOH was aspirated through the sensor while the cell resistance was recorded. After a significant change in resistance was established the Dynel disc and the screens were removed and flushed in a known quantity of distilled water. The KOH mass extracted from the stream was calculated from the pH change in the solution. A new disc was then mounted in the cell, and the experiment was repeated to establish another calibration point. A curve showing mass of entrained KOH vs. cell resistance was generated in this fashion. The data indicated that the cell would respond over a range from 10^{-7} gram to 10^{-2} gram of KOH.

The reproducibility of the KOH mass determination in the lower portion of the sensitivity range (10^{-5} gm to 10^{-7} gm) limited accuracy to an indication of the order of magnitude of KOH entrainment. With indicated entrainment greater than 10^{-5} gm, the maximum error would modify the sensor indication by a factor of 2 only. This performance was based on consideration of seven data points obtained under laboratory conditions. It is most probable that the generation of new calibration data, collected in place during cell operation, will show the sensor to be capable of greater resolution.

3.3 Gas Contamination Sensors

The use of a catalytic reactor was considered to be the most suitable means of detecting gas contamination. Comparison was made with spectrophotometric methods which, as with the detection of KOH entrainment, was eliminated by its complexity, size and cost.

A survey of standard catalytic reactors showed no commercially available unit of a size small enough for the analytical train geometry. A sensor was made in the laboratory by wrapping American Cyanamid AB6 electrode material around a thermistor. This device and an unmodified thermistor were placed in a tube and exposed to a stream of oxygen contaminated 1% by volume with hydrogen. The unwrapped thermistor was located upstream followed by the contamination-sensitive element. The second thermistor indicated a temperature rise in the catalytic bed proportional to the flow rate of the gas mixture and the percentage contamination. A controlled experiment showed no effect when pure oxygen flowed in the tube. The temperature rise in the contamination sensor correlated linearly over the range of flow rate and contamination relevant to the orbital experiment. A sensor based on this preliminary trial was incorporated in the analytical train.

3.4 Gas Flow Measurement

Two types of flowmeters were given serious consideration for the measurement of oxygen and hydrogen evolution rate. The types studied were the choked orifice and the laminar flow capillary tube. The laminar flow tube was selected on the basis of the advantages discussed below.

To insure that the pressure in the gas exit tubes will not fall much below one atmosphere, a pressure-dropping device will be needed between each and space vacuum into which the gases will exhaust. A flowmeter designed to produce a one atmosphere pressure drop at the expected flow would accomplish this purpose in addition to measuring the gas flow, thereby eliminating the need for an additional pressure-dropping device.

In the orbital experiment the electrolysis stack will electrolyze 6.3 grams of water per hour or 1.75×10^{-3} gm/sec. The corresponding flows of hydrogen and oxygen will be 1.95×10^{-4} gm/sec and 1.555×10^{-3} gm/sec respectively. Standard techniques* were used to calculate the sizes of the orifices and

*"The Dynamics and Thermodynamics of Compressible Fluid Flow", Volume 1, A. H. Shapiro, Ronald Press Company, New York, 1953, pp. 178-183.

capillary tubes required for this application, assuming an upstream pressure of one atmosphere. The values obtained for the required orifice diameters were 0.00247 inches and 0.00350 inches for hydrogen and oxygen respectively. The lengths calculated for 0.010 inch laminar flow capillary tubes were 9.52 inches and 8.35 inches for hydrogen and oxygen respectively.

Isothermal flow was assumed for the capillary tubes. The actual flow will probably be isothermal over most of the tubes, but adiabatic near the outlets. Since adiabatic flow would result in tube lengths about 10% longer than for isothermal flow, the procedure used in fabrication was to fabricate the tubes somewhat longer than was calculated for the isothermal flow condition. The tubes were then tried and cut to give the desired values.

Adjustment of the orifice diameter by removing material from the upstream face would be an extremely delicate process due to the small diameter involved. Possibly a more significant disadvantage of the orifice is that erosion or deposition could change the calibration by significant amounts, whereas the much greater wall area of the tube would not change significantly from these effects. An upstream filter would be required with either device to insure that the gas streams are free of particulate matter, although the orifice would be more subject to plugging than the larger diameter capillary tube. The orifice, being an adiabatic device, would also be more subject to icing than the nearly isothermal capillary tube.

In the final packages (See Section 4.0) the tubes were serpentined for compactness and clamped to the stack end plates to provide as nearly an isothermal condition as possible. Using tube diameters of 0.0115 inches, the computed tube lengths were 11.2 inches and 13.3 inches for hydrogen and oxygen respectively. The final adjusted lengths were 9.8 inches and 11.75 inches for hydrogen and oxygen respectively.

In order that the flows reach the critical condition, the required downstream pressures were computed to be 0.74 psia and 1.1 psia for hydrogen and oxygen respectively. Particular attention had to be directed to the downstream plumbing configuration in order that the pressures at the discharge ends of the capillary tubes not exceed these values.

3.5 Instrumentation Electronics

The instrumentation electronics package contains signal conditioning circuits for fourteen (14) sensors:

Four entrainment sensors (two in each gas stream)
Two contamination sensors
Two gas temperature sensors
Two gas humidity sensors
Two gas pressure sensors
One cell stack temperature sensor
One water supply pressure sensor

The measurements of the three cell voltages and the cell current do not require signal conditioning on the experiment side of the telemetry interface.

The active component of each sensor is arranged as an element of a resistance bridge network. A 2 KC inverter and voltage regulator are included in the package, and supply each bridge with a square wave voltage. The bridge outputs (with the exception of the pressure sensors) are demodulated and applied to dual emitter-follower circuits which provide signals nominally 0 to $\pm$ 1 VDC into a 100,000 ohm impedance. The outputs of the pressure transducers are not processed by the electronic package, and pressures are indicated by signals in the range 0 to 50 mv DC at the telemetry terminals.

The signal conditioning components are mounted on four (4) printed circuit boards, which fit into a package of approximately 4" x 4" x 3 1/4". A relay is employed to switch four time sharing circuits at two (2) second intervals. These circuits are incorporated to reduce package complexity and weight. The electronics package operates off an external power source of 12 VDC.

4.0 UNIT DESIGN AND FABRICATION

A photograph of the Electrolysis Cell System for Orbital Test is shown in Figure 4-1. The unit is mounted on a vibration test fixture plate in this photograph. The major unit subassemblies visible are the electrolysis cell stack, the water reservoir, the instrumentation electronics package and the mounting structure. The analytical trains are mounted on the stack end plates and are covered by the end plate assembly thermal radiation shields.

A system block diagram is shown in Figure 4-2. The effluent gases from the cells flow through the analytical trains and capillary tubes and are vented to vacuum. Makeup water is fed to the cell stack from the water reservoir to replace the water consumed by electrolysis and lost by evaporation. Manually operated valves are used in ground operation and are capped prior to launch. To start the unit after orbital injection, it is necessary only to supply power to the cell stack and instrumentation and to open the three explosive valves.

The following subsections describe the design philosophy utilized in fabrication of the flight unit and summarize the unit design point specifications.

4.1 Unit Design Philosophy

4.1.1 Electrolysis Cell Stack

A cross section of the stack is shown in Figure 4-3. A unit cell consists of a KOH/oxygen bi-polar plate (3) and a hydrogen plate (4, 34). Two recesses and a pin structure cavity are provided on the KOH side of the bi-polar plate. (See also Figure 4-4). The cavity communicates with the electrolyte manifold via a drilled hole in the plane of the plate. A length of TFE spaghetti tubing (10), etched on the outside for adhesion, is inserted into the hole and extends into the manifold. The other end of the tube extends to a point just short of the opposite end of the cavity. The entire sleeve is secured in place with epoxy adhesive. This tube intersects the manifold TFE liner sleeve (8) which is epoxied into place prior to the installation of the smaller tube. The manifold liner sleeve extends slightly beyond the surface of the metal plate in order that a tight, butt contact will exist between all liquid manifold sleeves.

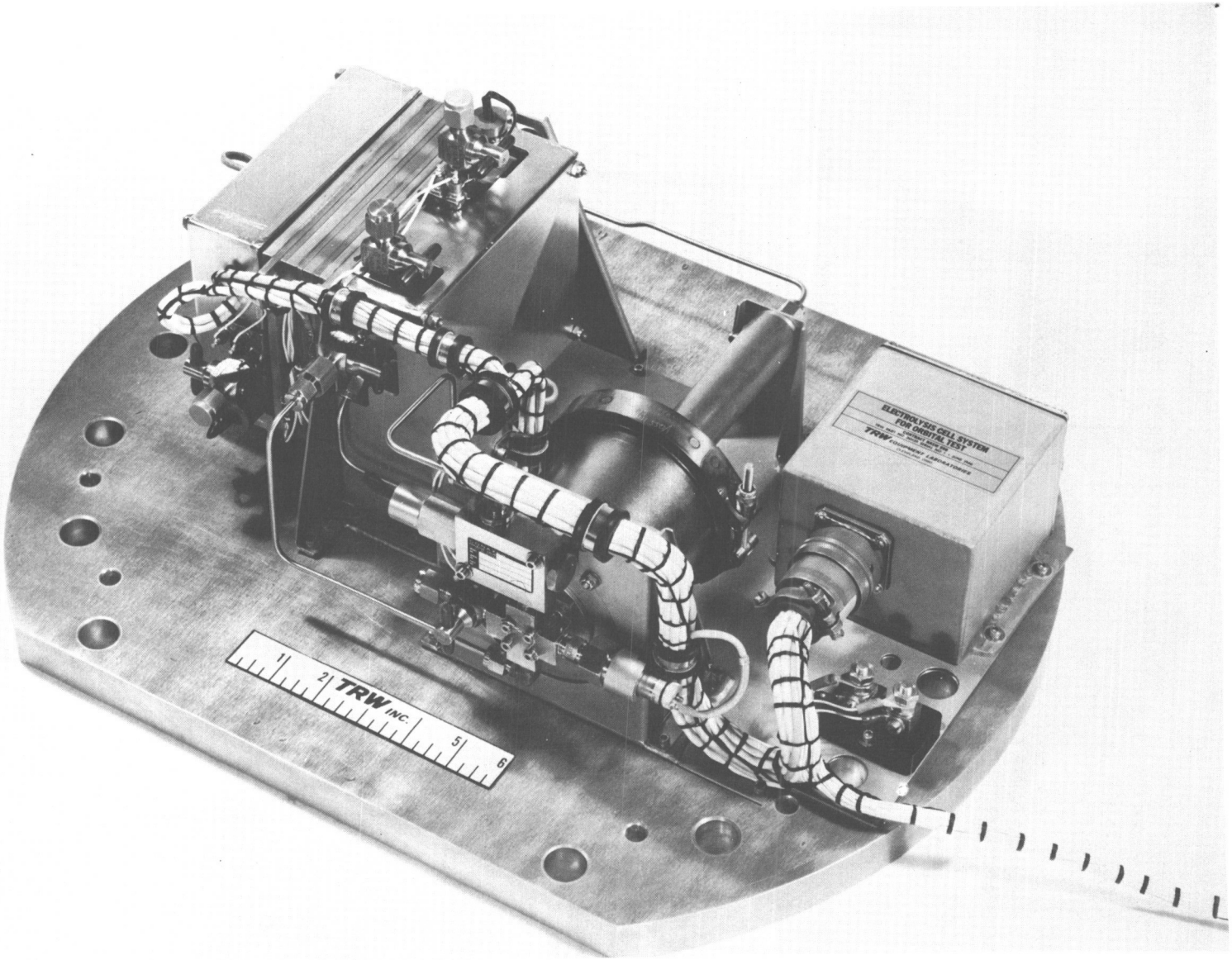

FIGURE 4-1 ELECTROLYSIS CELL SYSTEM FOR ORBITAL TEST

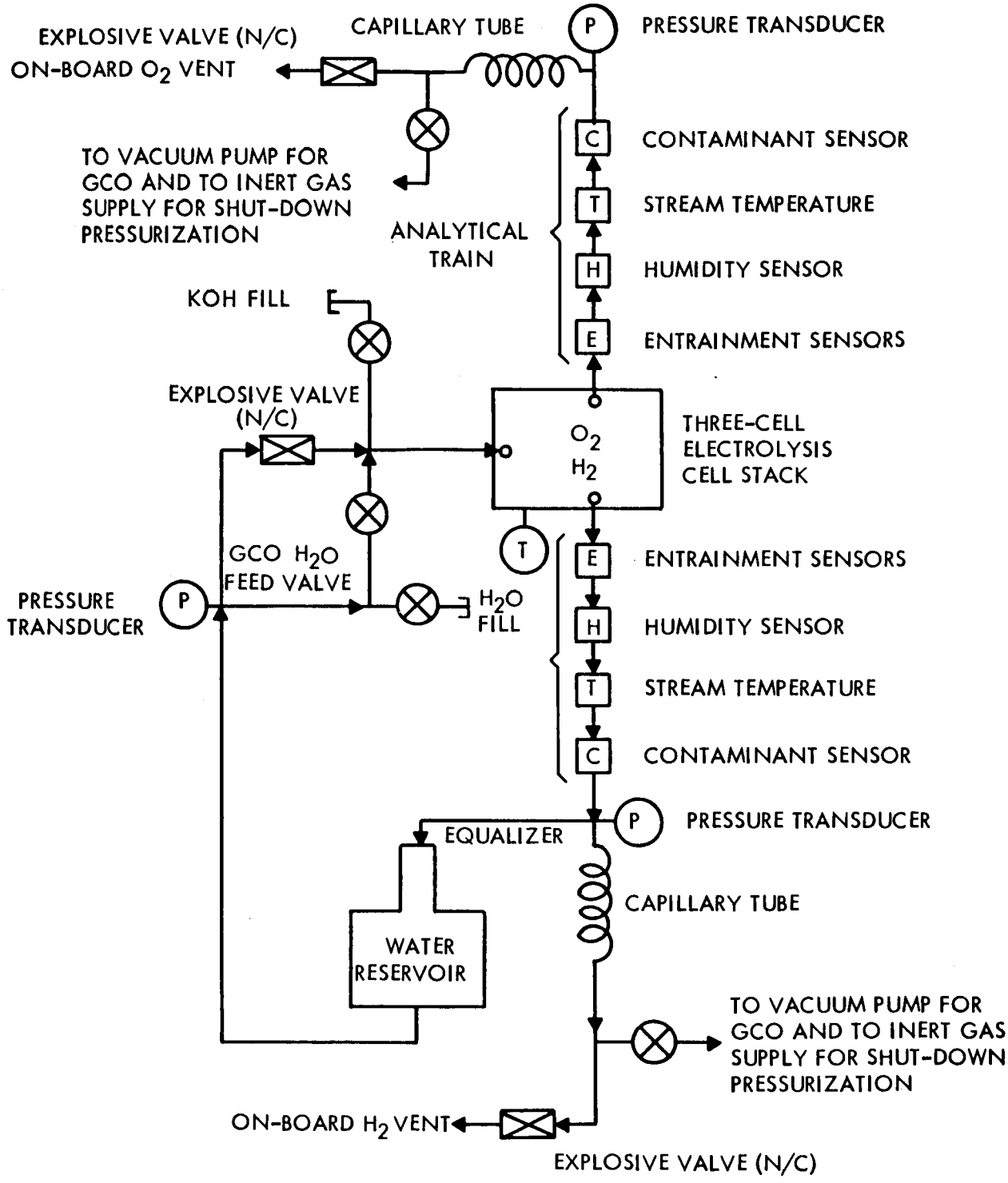

FIGURE 4-2 SYSTEM BLOCK DIAGRAM

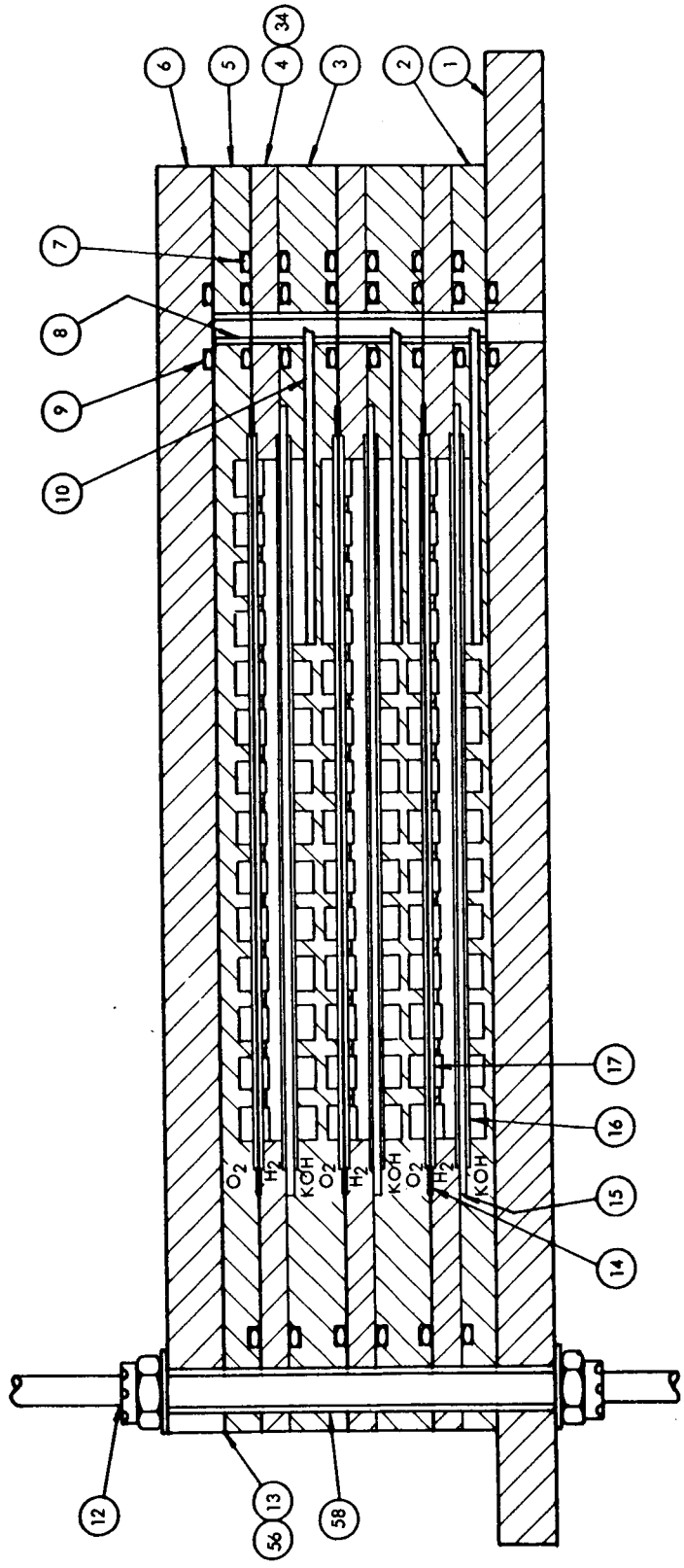

FIGURE 4-3 CROSS-SECTION OF ELECTROLYSIS CELL STACK

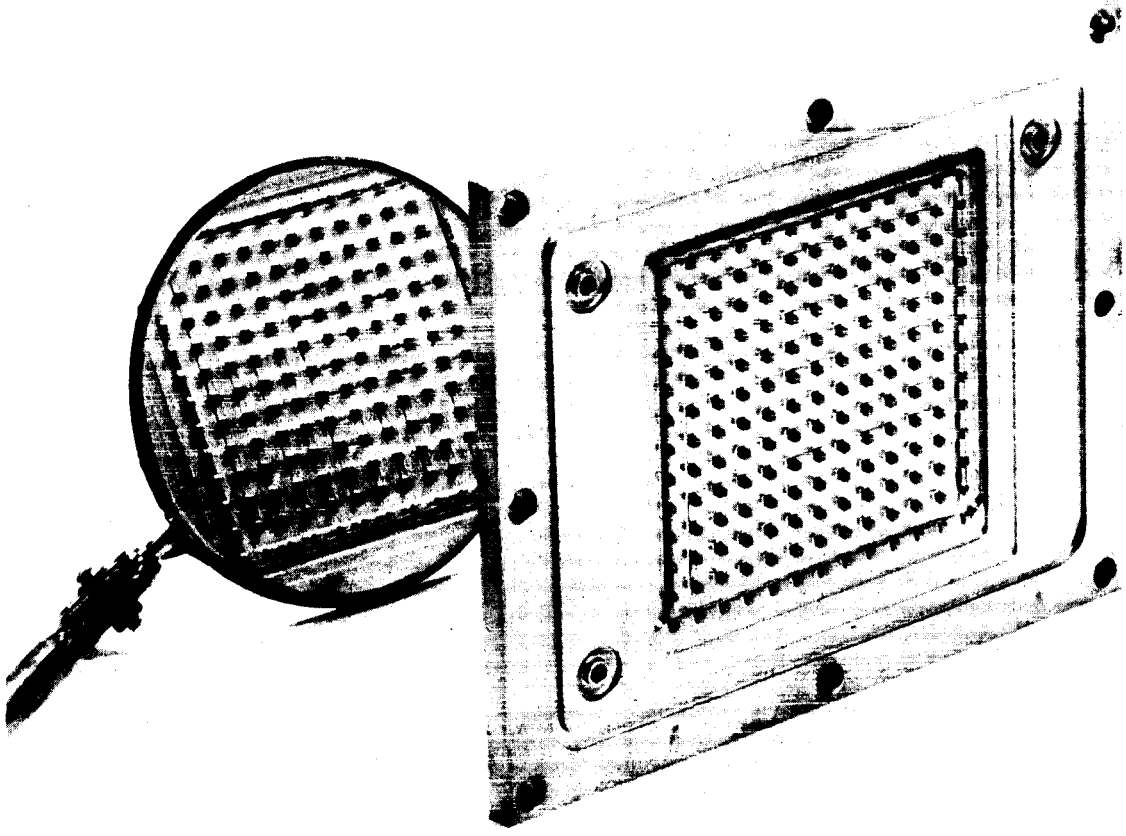

FIGURE 4-4 KOH/OXYGEN SUB-ASSEMBLY BI-POLAR PLATE

The use of the sleeves and tubing provides a feed path of high ohmic resistance in order to insure that electrolysis between cells via the feed tubes is minimal. Due to the very small volume of electrolyte contained in the feed tubes, a relatively short period of stack operation will serve to sweep the tubes clear of electrolyte with feed water, thereby further reducing the rate of inter-cell electrolysis.

The first recess in the KOH plate serves to accommodate the feed matrix support screen (16). The second recess accommodates the feed matrix (15).

The hydrogen plate (4) has a 3 in. x 3 in. open window area and recesses on both sides at the edge of the window. (See Figure 4-5). The window area communicates with the hydrogen manifold via a drilled hole in the plane of the plate. The recess on one side of this plate accommodates the other support screen (16) for the feed matrix when the plates are mounted against each other. The opposite face of the hydrogen plate is provided with a film of FEP (13) and adhesive film (56) in order to bond the film to the plate. The inside dimensions of the film form a second recess on this side. The smaller recess accommodates the hydrogen electrode (17) and the larger recess, formed by the FEP film, accommodates the cell matrix (14).

The window section of the hydrogen plate is equipped with a machined screen structure (34) with the intersections of each machined wire in alignment with the pins in the adjacent plate cavities. This structure permits free diffusion of water vapor from the feed matrix to the cell matrix, free lateral flow of the evolved hydrogen to the exhaust port and also augments the electrical conduction path from the face of the electrode to the hydrogen plate.

The face of the hydrogen plate is mounted against the oxygen side of the bipolar plate, which in turn is equipped with a pin structure cavity, a drilled port into the oxygen manifold, and a single recess. This recess accommodates the oxygen electrode (17), the last remaining component in the unit cell.

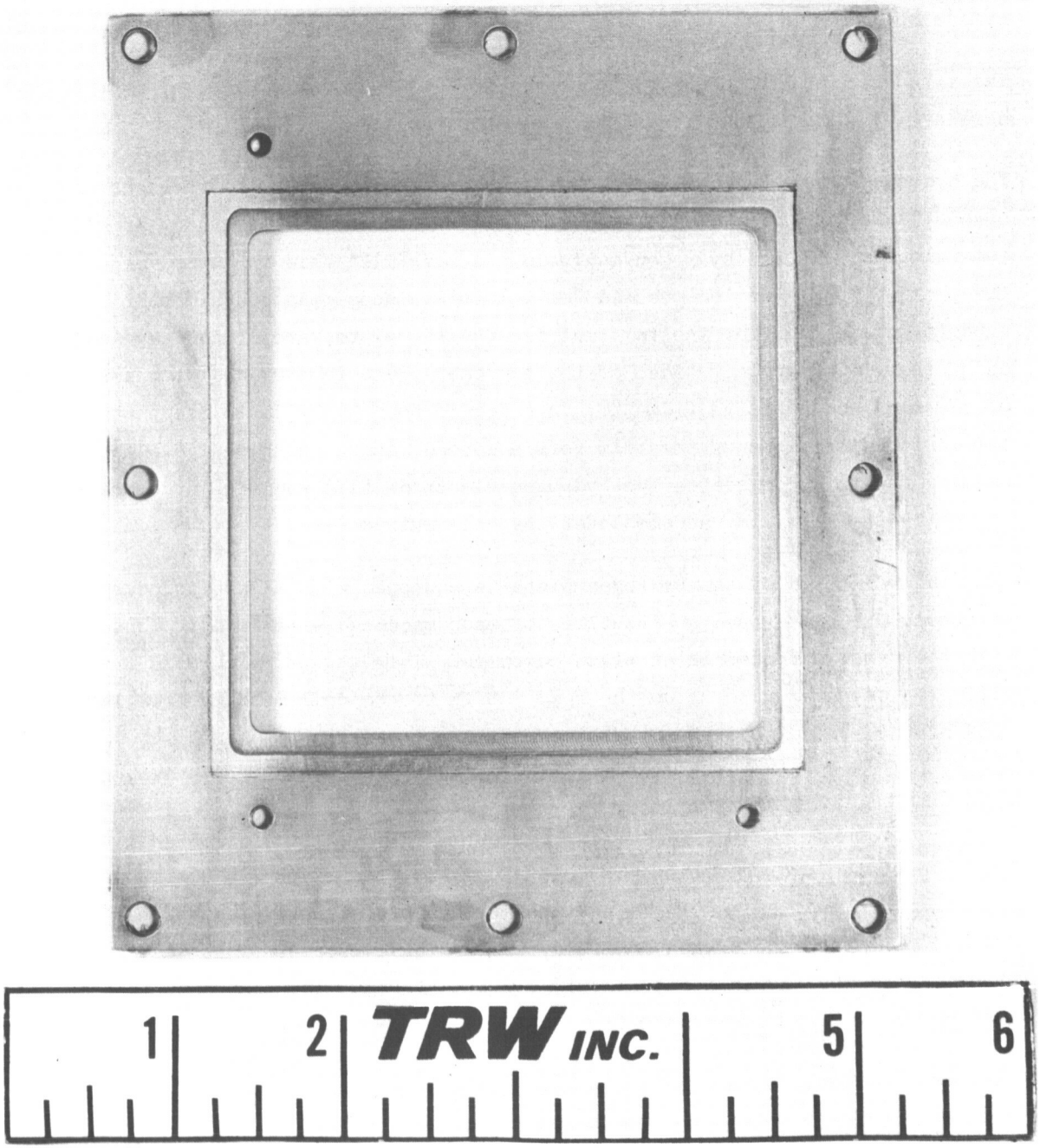

FIGURE 4-5 HYDROGEN SUB-ASSEMBLY PLATE

Three such cells are stacked together (See Figure 4-6) with the last plate on one end of the stack (2) comprising a KOH cavity only and the other (5) an oxygen cavity only. The plane back surfaces of these two plates are provided with a continuous FEP film in order to insulate these plates from the structural end plates, (1) and (6). These plates, (2) and (5), are equipped with current tabs for the stack. These and the bi-polar plates (3) are drilled at the edges in order to receive screws for attachment of voltage sensing leads.

The above assembly is confined within the structural end plates. These units support the analytical trains, capillary flow meters and control valving. One end plate has three sides extended for mounting purposes.

The entire assembly is bolted together with eight draw bolts (12). These bolts are covered by insulating sleeves (58) in order not to electrically short circuit the stack. These bolts extend on both sides to serve as supports for the radiation shields. The completed assembly (without the radiation shields) is seen in Figure 4-7.

Ethylene - propylene O -rings, (7) and (9), are used throughout for sealing the gas manifolds and cell perimeters. This material is resistant to hot KOH.

Both the FEP film and adhesive film were thoroughly evaluated for performance in hot KOH solution before acceptance for use in the stack. All the plates were fabricated from magnesium and electroplated with nickel and gold. The electroplate passed rigid tests for adhesion and porosity.

Since the gas streams are partially saturated with water vapor, it is necessary to maintain the gas flow systems, including the analytical trains, gas pressure transducers and capillary tubes, heated to stack temperature; consequently, these components were mounted to the stack end plates. These components were either gold plated or covered with gold plated mounts in order to minimize radiation losses. In addition, a gold plated, thermal radiation shield was mounted over each end plate.

Heat removal from the stack was provided via conduction through the mounting flange and support structure. (See Figure 4-1.) In turn, the support

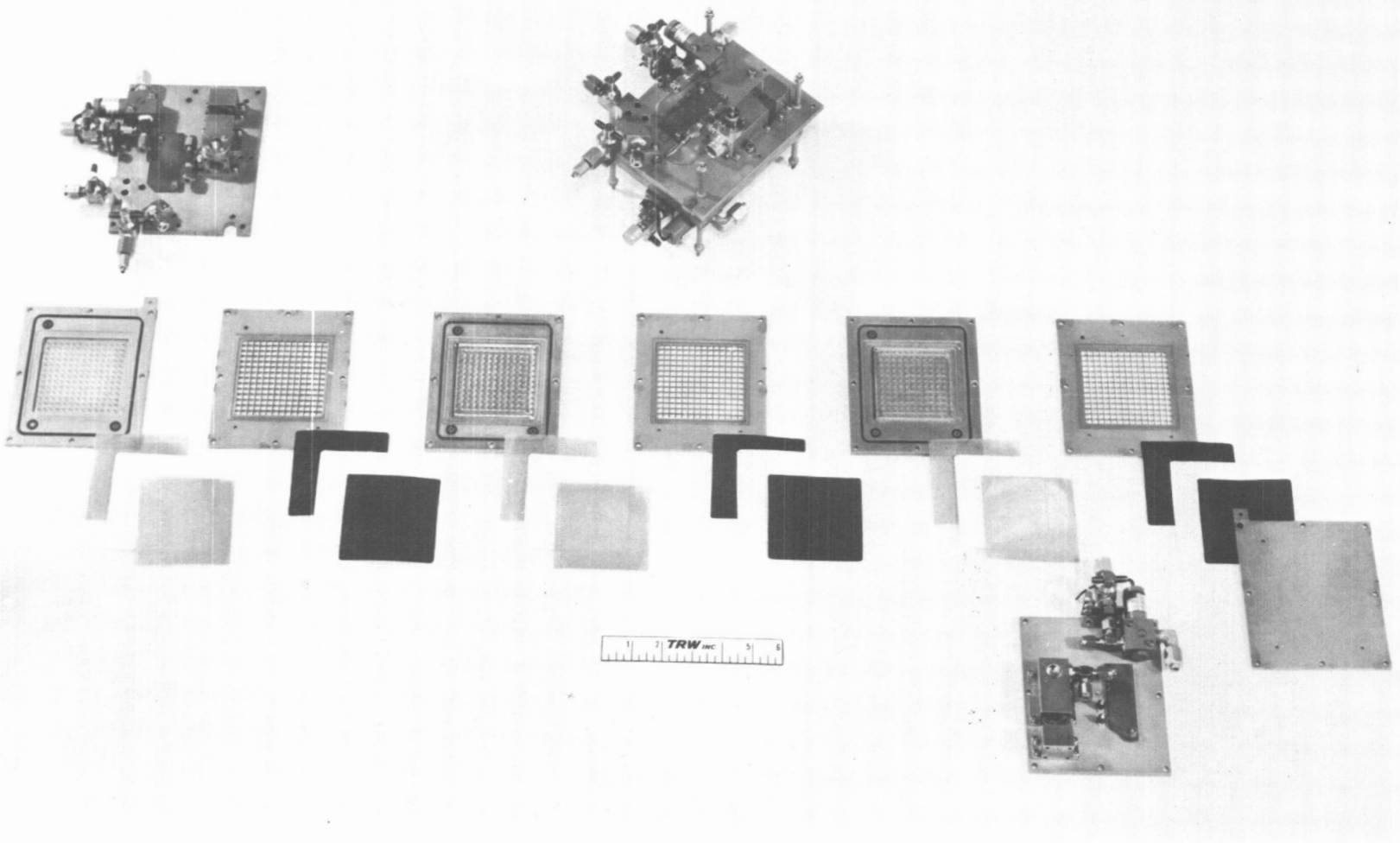

FIGURE 4-6 COMPONENTS FOR THREE-CELL STACK

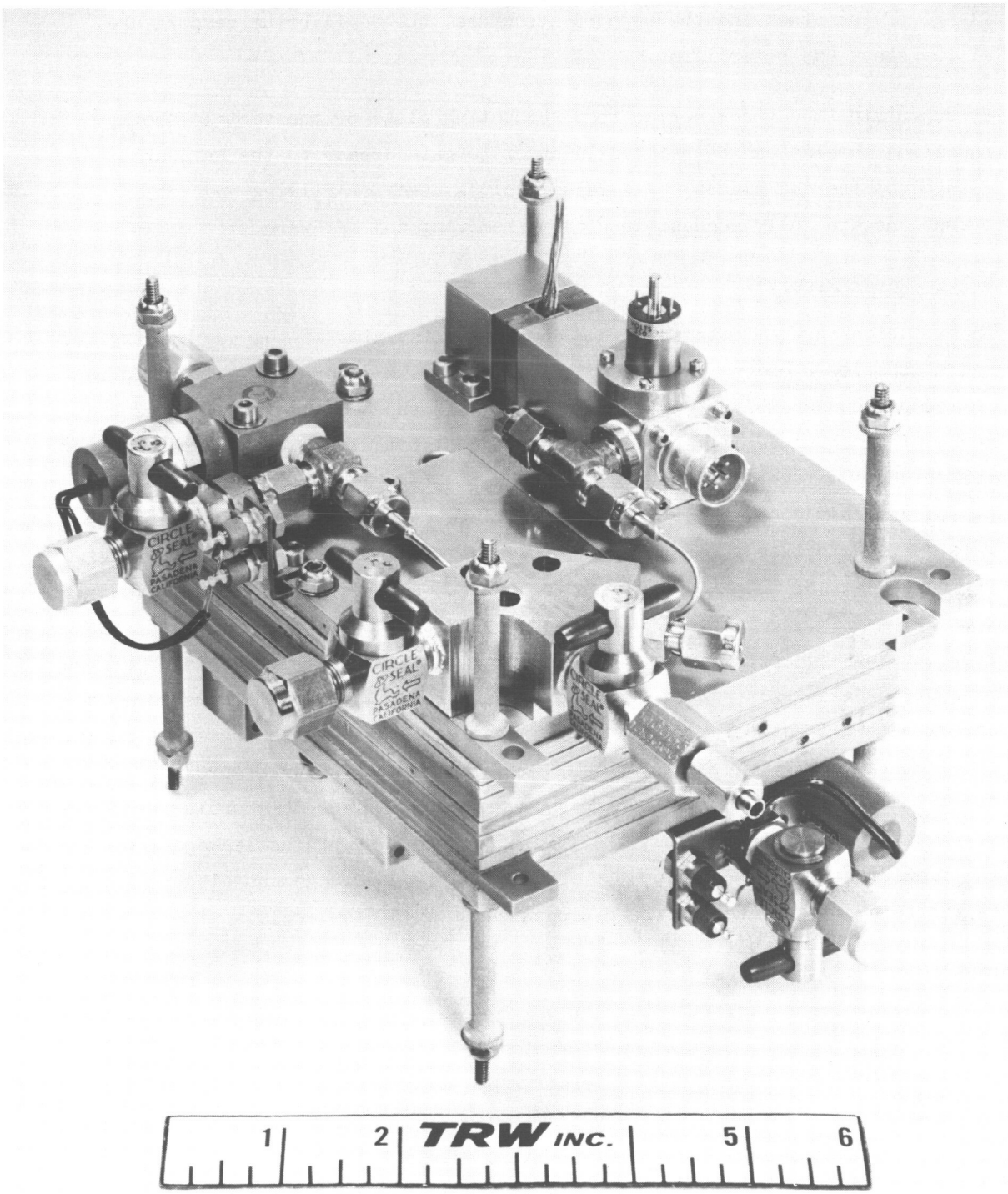

FIGURE 4-7 ELECTROLYSIS CELL STACK ASSEMBLY

structure will be mounted to a rigid, thermally controlled plate on the vehicle. By varying the geometry and type of thermal insulation between the mounting flange of the stack and the support structure, the equilibrium temperature of the stack can be modified.

By supporting the stack normal to the mounting plate of the vehicle, both radiation shields can be removed in order to gain access to the hardware mounted on the end plates. All manual valves used for filling and venting operations are fully accessible without removing any hardware.

4.1.2 Water Reservoir

An extension spring fastened at one end to the interior of the top housing, and at the lower end to the piston anchor, serves to maintain an upward force on the piston assembly. (See Figure 4-8.) The top housing is connected by means of an equalizer line to the hydrogen outlet manifold thereby referencing the pressure on the top of the piston assembly to the hydrogen pressure. The piston assembly consists of the retainer plate, piston and rolling diaphragm. This design provides a zero leakage piston with very little piston restraint. During operation, the liquid system is continuous between the reservoir and the feed matrix of each cell. Assuming the piston to be off of the top end stop, the upward spring force maintains the liquid pressure below the hydrogen pressure at all times. With the water reservoir full, the water pressure is approximately 1 psi below the hydrogen pressure. When all the water is consumed by the cells, the spring is fully extended, and the water pressure is approximately 3.5 psi below the hydrogen pressure. Since the bubble pressure of the feed matrix is 52 psid, there is no possibility of gas leakage into the feed compartments. Due to the reference spring arrangement electrolyte is restrained from entering the hydrogen cavities of the cells.

Launch considerations require that the thrust axis lie parallel to the axis of the water reservoir, with the top of the reservoir in the forward direction of motion if the system is to be operational during launch. In this position, the water in the reservoir is at negative hydrostatic head with respect to any area of the feed matrix. Therefore launch acceleration will not displace water from the reservoir into the gas cavities within the stack. The negative

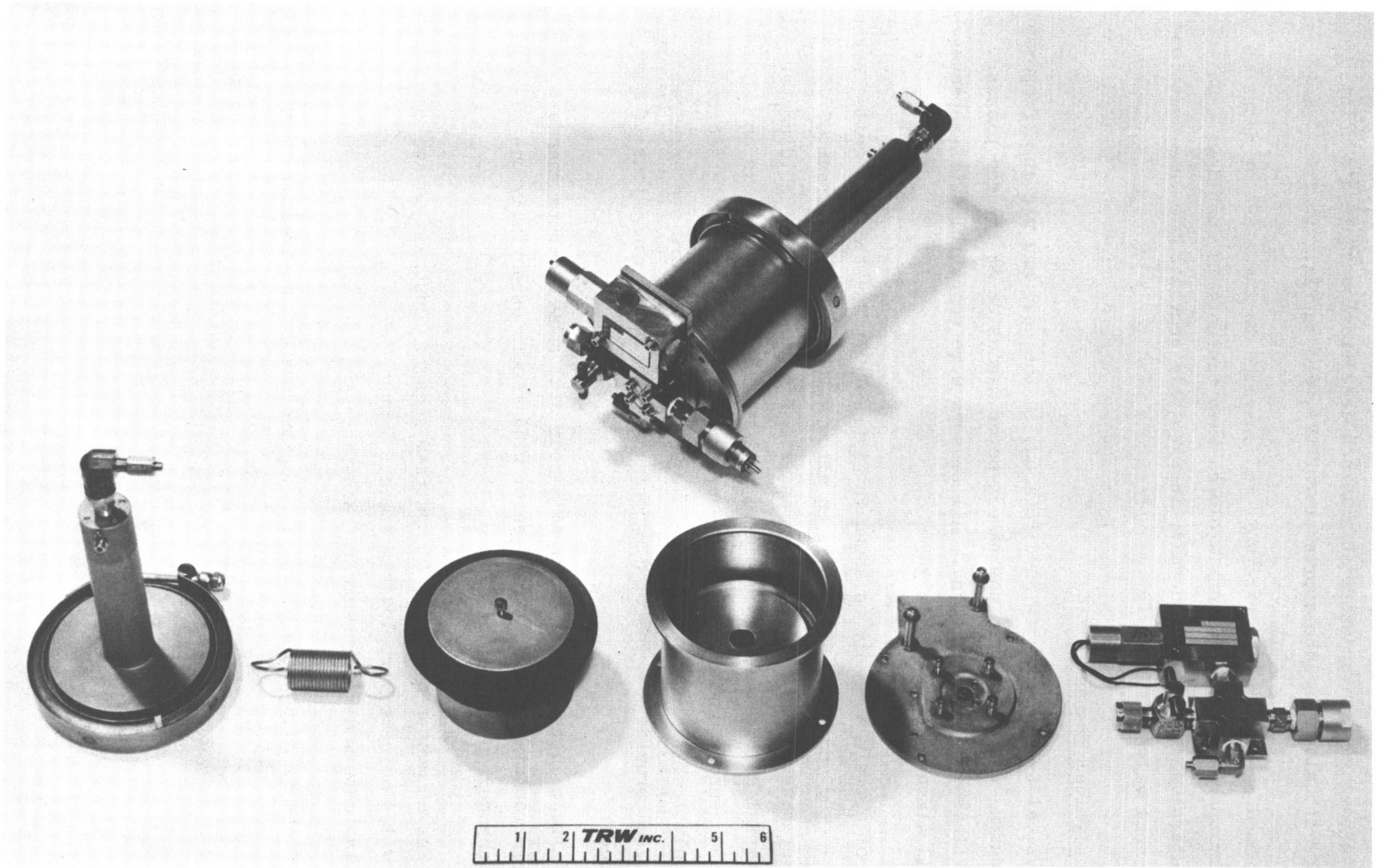

FIGURE 4-8 WATER RESERVOIR COMPONENTS

hydrostatic head at the top end of the feed matrix will reach 4.5 psi with respect to the hydrogen pressure at a launch acceleration of 15 g's. This value is well below the bubble pressure of the feed matrix.

During ground check out, the reservoir is connected to the stack by means of a manually operated valve, which is closed when the unit is shut down. On orbital start-up, the explosive valve is fired and provides the same function as the manual valve.

4.1.3 Analytical Trains

The analytical trains were designed to mount on the cell end plates. Components of the housing were made from the same type of magnesium as the end plates and were finished by gold plating. All sensors were compatible with a package of overall dimensions 1" x 1" x 3".

A sketch of a train assembly is shown in Figure 4-9. Gas from the cells leaves the port in the end plate and enters an elbow which turns the stream 90°. Entrainment sensors are first in line and are formed by 0.437 inch diameter Dynel material held between gold plated screens. Figure 4-10 shows an entrainment sensor housing, a pair of screens and the two metallic sections of the analytical train housing. The two entrainment sensors are arranged in series and provide a means of diagnosing the following conditions if they should occur:

a) Slight entrainment. Upstream sensor will show moderate change in resistance; downstream sensor will remain essentially unchanged in resistance.

b) Entrainment penetration of upstream sensor. Upstream sensor will indicate very low resistance; downstream sensor will indicate moderate change in resistance.

c) Gross flooding of electrolyte. Upstream and downstream sensors will indicate very low resistance.

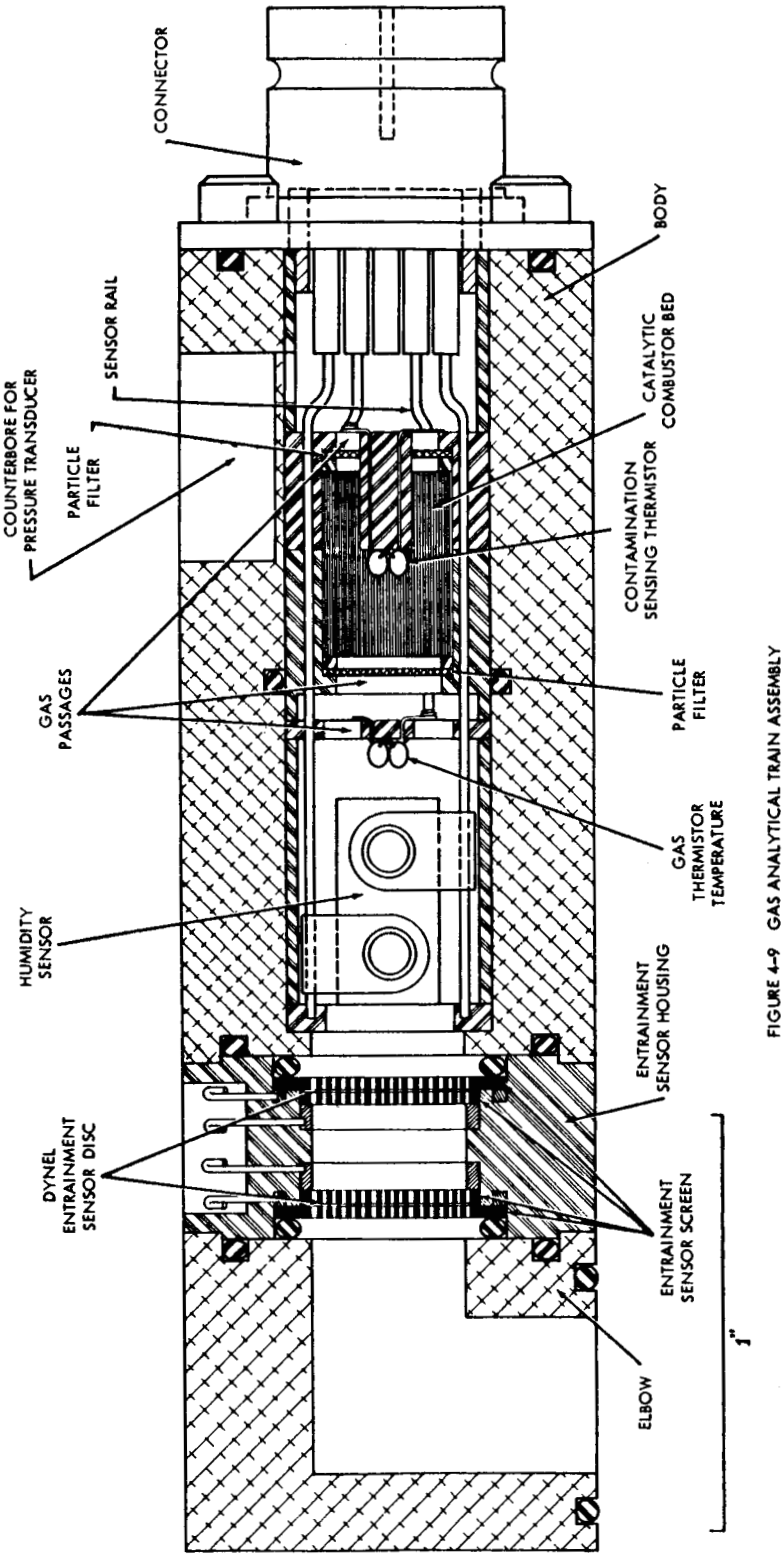

FIGURE 4-9 GAS ANALYTICAL TRAIN ASSEMBLY

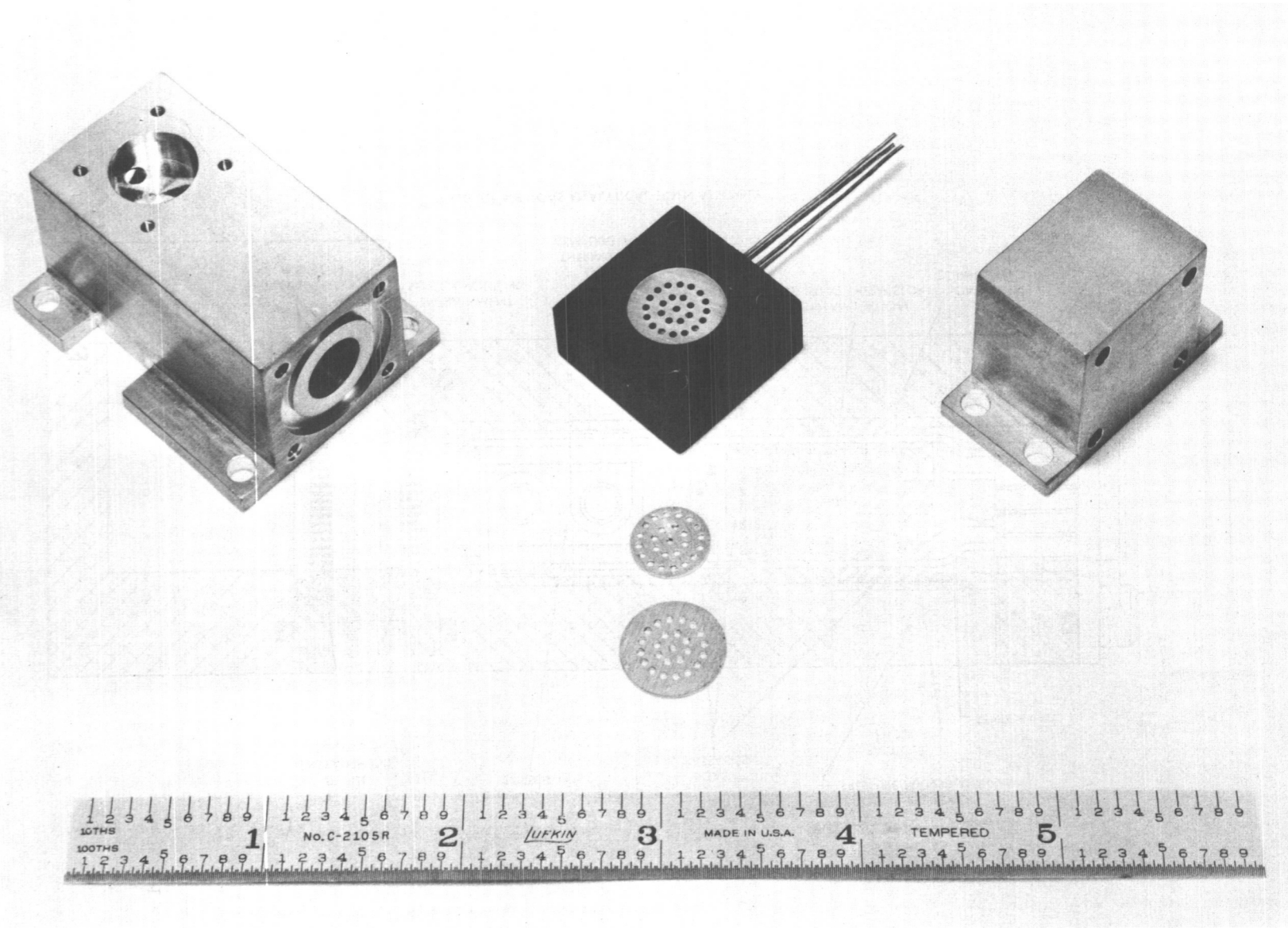

FIGURE 4-10 ANALYTICAL TRAIN HOUSING AND ENTRAINMENT SENSOR

The sensors are mounted in a hermetically sealed epoxy housing which is inert to KOH. Contact rings which form seats for the screens are machined to create up to 15% compression in the Dynel in order to ensure good contact with the screens. Both entrainment sensors may be removed to allow KOH mass determination after exposure to entrainment.

Three in-line sensors are mounted in a hermetically sealed epoxy structure. Connections to the sensors were made via rails molded integrally with the sensor mounting components. The analytical train structure is essentially a hollow cylinder in which spacers and sensor subassemblies were stacked in turn starting at the 7-pin connector. Spacers and housings for the sensor subassemblies were machined from epoxy bar stock of the same composition as the epoxy used to cement the elements together. Figure 4-11 shows the components for the in-line subassembly ready for assembly. Shown from right to left are:

a) Connector with soldering rails in position.
b) Spacer with holes communciating gas stream to pressure transducer and capillary port.
c) Lower half of contamination sensor with thermistor and filter subassembly in place.
d) Top half of contamination sensor with filter in place.
e) Stream temperature subassembly with thermistor and mounting platform.
f) Humidity sensor housing.
g) End cap.

The in-line subassembly passes through an O-ring in the analytical train housing which constrains flow to passages cut in the mounting components. Gas flow through the sensors is in the following order:

a) Humidity
b) Gas temperature
c) Catalytic combustor to detect gas contamination

Particle filters were mounted in each end of the contamination sensor to prevent platinum from the catalytic bed from blowing into the capillary tube.

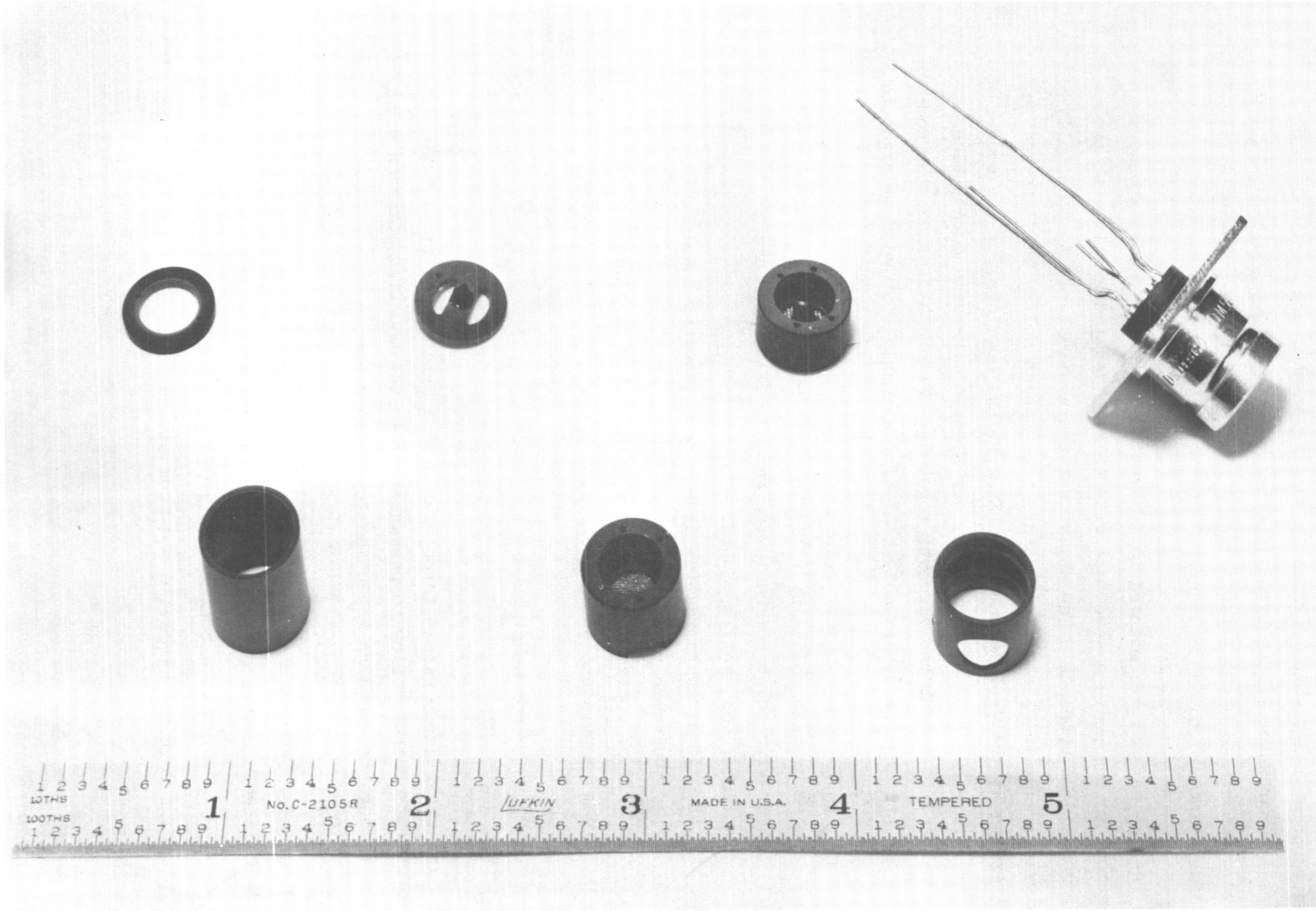

FIGURE 4-11 COMPONENTS FOR ANALYTICAL TRAIN IN-LINE SUB-ASSEMBLY

The pressure transducer is mounted on the analytical train housing above the plenum chamber just upstream of the flow metering capillary. A view of a completely assembled oxygen analytical train was shown in Figure 4-7.

4.1.4 Mounting Structure

The electrolysis stack and water reservoir are mounted off the backing plate by gusset plates. All support will be derived from the backing plate which has been assumed to be completely rigid (similar to the mounting surface of the "01" Standard Payload Module). This arrangement provides a very rigid support for these components. The electronic package and current shunt will be mounted directly to the backing plate. The back plate of the mounting structure serves no purpose other than to maintain all components in the proper relationship to each other. Throughout the entire system vibration proof nuts, lock wiring or screw lock thread inserts were used. The screw lock thread inserts were used in all the magnesium components to prevent thread stripping.

All materials were selected for maximum corrosion resistance to the liquids involved. Corrosion couples were avoided by protective electroplates of the same noble metal, gold in most instances. The aluminum supporting structure was nickel plated to prevent damage in the event of accidental spillage of electrolyte.

4.2 Unit Specifications

The design point specifications for the unit are listed in Table 4-1.

TABLE 4-1

Unit Design Point Specifications

Current density	= 100 amperes/ft^2
Area (per cell)	= 0.0625 ft^2
Current	= 6.25 amperes
Electrolyte concentration	= 32% KOH (by weight)
Cell temperature	= 140°F
Hydrogen cavity pressure	= 14.7 psia
Oxygen cavity pressure	= 15.7 psia
Cell voltage	= 1.57 volts
Stack voltage	= 4.71 volts
Mass flow rate of dry oxygen	= 0.0123 lb/hr
Dew point of gases	= 118.5°F
Humidity ratio of oxygen	= 0.065 lb H_2O/lb O_2
Mass flow rate of wet oxygen	= 0.0131 lb/hr
Density of oxygen/water vapor mixture	= 0.0746 lb/ft^3
Volumetric rate of oxygen/water vapor mixture	= 0.176 CFH
Mass flow rate of dry hydrogen	= 0.00153 lb/hr
Humidity ratio of hydrogen	= 1.11 lb H_2O/lb H_2
Mass flow rate of wet hydrogen	= 0.00323 lb/hr
Density of hydrogen/water vapor mixture	= 0.0087 lb/ft^3
Volumetric rate of hydrogen/water vapor mixture	= 0.371 CFH
Gas humidification rate, oxygen gas	= 0.000801 lb/hr
Gas humidification rate, hydrogen gas	= 0.00169 lb/hr
Water decomposition rate	= 0.0139 lb/hr
Water consumption rate	= 0.0164 lb/hr
Weight of water consumed in 24 hrs	= 0.393 lb
Volume of water consumed in 24 hrs	= 10.9 in^3
Volume provided in water reservoir	= 14.4 in^3
Cooling load on cold plate imposed by stack	= 19.3 BTU/hr (maximum)

5.0 UNIT TESTING

Prior to delivery of the Electrolysis Cell Unit, it was subjected to a 24 hour performance test. Three objectives were associated with this test:

a) Successful completion of a continuous 24-hour test establishing feasibility of a compact, multi-cell, wick-vapor-feed electrolysis system for subsequent orbital test.

b) Establishment of detailed procedures covering all phases of pre-test, test, and post-test operations.

c) Verification of instrumentation operation and, using the unit as a test bench, calibration of the entrainment sensors.

5.1 Performance Acceptance Test

Following the charging of KOH into the three cell stack and water into the reservoir, the start of the test was delayed several days when it was discovered that electrolyte had been inadvertently forced into the oxygen instrumentation train. This was determined when the sensor signals failed to provide reasonable data during the final checkout preceding the twenty-four hour test. The trains were removed and a series of detailed checks were performed in search of any possible internal cell leaks. None were found. It was concluded that the reason for the KOH having entered the train was an incomplete purging of the gas cavities following the initial charging of the stack with electrolyte. The charging procedure was subsequently modified to avoid a recurrance of this problem. The result of the KOH bath (which apparently lasted nearly seventy-two hours) was that the conducting layer on the humidity sensor was dissolved, leaving it to register as an open circuit. Washing the analytical train in distilled water and baking dry alleviated shorting of the temperature sensors to the train housing. Since replacement of the humidity sensor entailed cutting apart the stycast housing, it was decided to run the twenty-four hour test without the benefit of an operable oxygen humidity sensor. Therefore, the analytical trains were replaced, and, at 1420 hours on 20 May 1966, the test was initiated on Serial No. 2 unit. Water aspirators were used to evacuate the hydrogen and oxygen exhaust lines. The cell stack proper was wrapped with approximately a one-inch blanket of insulation to minimize any convective cooling that might occur, the object here being to allow the cell the best possible

chance of reaching design temperature of 140°F without using an oven or vacuum chamber.

The first item that became apparent was that, at the reduced cell operating temperature following startup, the voltage required was a good deal less than expected in order to maintain a current density of 100 ASF. The performance improvement over that displayed by earlier prototype cells was credited to the new gold plated hardware and electrodes. The slow increase in cell temperature experienced after startup made it doubtful that 140°F would be reached. This proved to be true; the highest temperature achieved during the twenty four hour test was 98.6°F. Even so, the cell voltage requirement remained in the 1.65-1.70 volts range. The current density was controlled to 100 ASF $\pm$ 0.33 ASF for the entire test duration.

At slightly over seven hours of testing, the water reservoir pressure began to rise slightly relative to the hydrogen reference pressure. This was contrary to the expected mode of operation. The increase continued until, at just under nine hours operation, the water pressure was approximately equal to or slightly greater than the hydrogen pressure. This was indicative of a leak some place in the system. The possibilities included 1) a leak in a feed matrix thus allowing gas passage, 2) a leak across or through the bellofram in the water reservoir or 3) a water reservoir leak to atmosphere. The attitude of the unit during test (water reservoir in the vertical position) was such that water reservoir pressure in excess of hydrogen cavity pressure by a few inches of water could be tolerated. However, much more than that would result in electrolyte entering the hydrogen cavities with possible damage to the gas stream instrumentation. For this reason, after about thirteen hours of testing, in an effort to drive the hydrogen pressure significantly above the water pressure, the hydrogen exhaust pressure was increased by reducing the aspirator water flow. However it appeared as though the water pressure followed the hydrogen pressure, thus lending weight to the possibility of a system leak. After operating in this fashion for approximately four hours, the aspirator was readjusted to again provide maximum exhaust vacuum. During this entire test procedure the entrainment sensors gave no indication of electrolyte entrainment.

The system ran quite smoothly until a little over twenty-three hours when the voltage on cell three began to increase. At twenty-three hours fifty five minutes it reached a peak of 1.7525 volts, the highest voltage recorded during the test. Twenty minutes later it had dropped to 1.7310 volts. Simultaneously with the voltage increase, the gas cavity pressures dropped slightly, and the cell stack temperature rose. The conclusion drawn from these indicators was that water was not being fed to the cell in question, which was the most remotely located from the water reservoir. Cell voltage remained near the 1.73 level for the last forty-five minutes of operation.

After twenty-four hours forty minutes of continuous running, system shutdown was accomplished. The significant test data accumulated during the run are shown in Figure 5-1. The trends of the stream and contamination temperatures (not shown) were much the same as the stack temperature.

During post-test checkout, it was discovered that the unit water inventory was down to its last forty grams of water, lending substance to the theory that the last cell may not have been getting the required amount of water. Further, the possibility of any real cell difficulties were discounted by an extensive leak check procedure conducted after the test. No internal cell leaks were found, either gas-to-gas or gas-to-liquid. Furthermore, the water reservoir was subjected to a sixteen hour pressurization with hydrogen with no indication of leakage. It is believed that some small leak was experienced during the testing, as indicated by the water reservoir-hydrogen pressure relationship, but it apparently did not exist once the test was completed. It could have been reseating of the bellofram or a particular O-ring. At any rate, post-test operations yielded no detectable leak.

The use of the system as a controlled test bench for calibrating the predoped entrainment sensors showed much promise. As discussed in Section 3.2, some information was gathered, but owing to the lack of more data, no trend was established. Continuation of this calibration procedure in future testing is suggested.

The oxygen analytical train was disassembled, and the humidity sensor was replaced and given a continuity check. After draining residual KOH from the cell stack

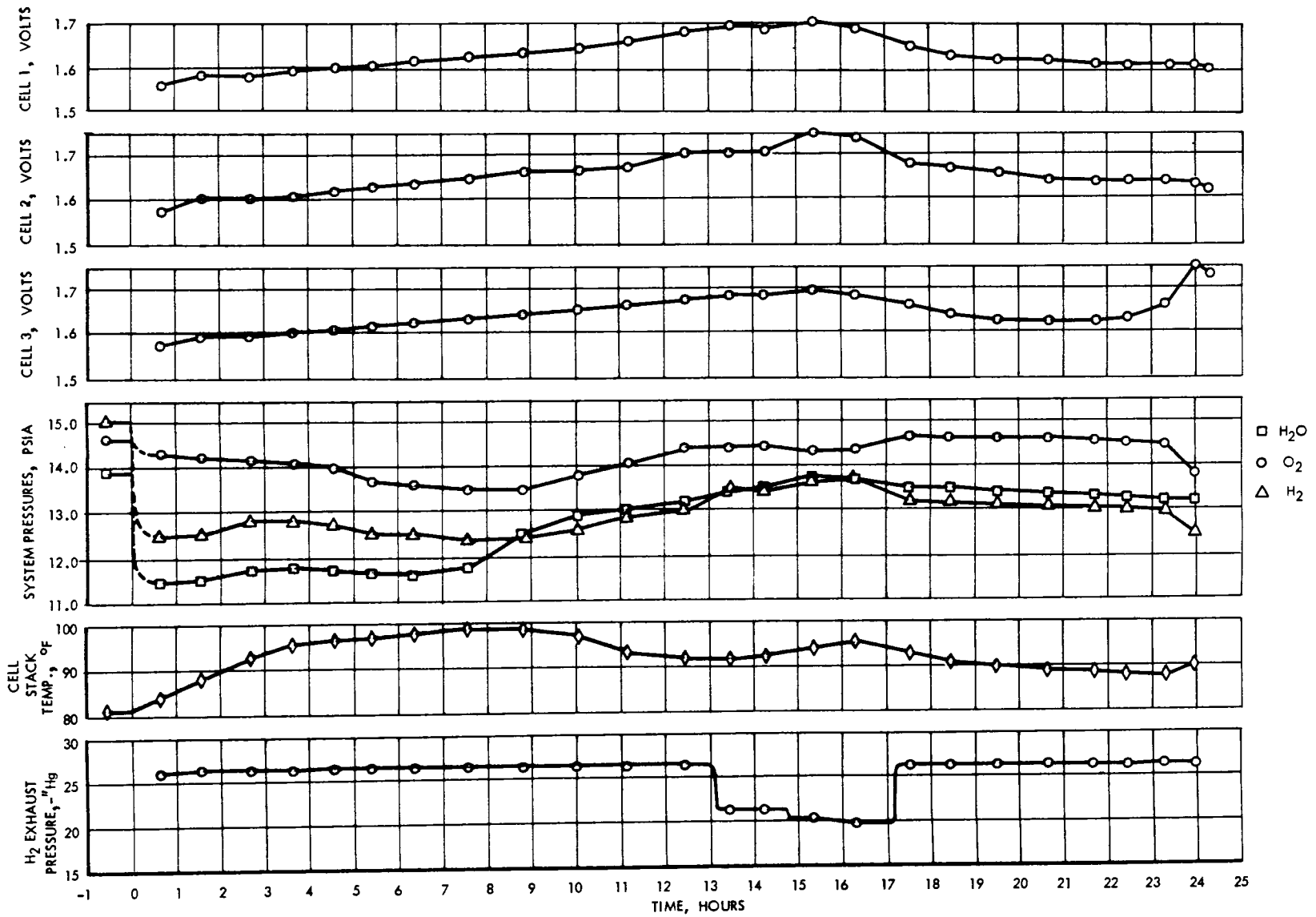

FIGURE 5-1 PERFORMANCE ACCEPTANCE TEST DATA

and placing a protective rubber gasket over the stack gas ports, the analytical trains were replaced, and the units were prepared for shipment.

6.0 CONCLUSIONS AND RECOMMENDATIONS

Feasibility has been demonstrated, under laboratory conditions, for a compact, high performance water electrolysis subsystem utilizing the wick-vapor-feed concept. This concept utilizes no dynamic components. It is recommended that work proceed on arrangements for the orbital test on one of the two packages to verify that no degradation occurs under actual gravity-free conditions.

It is further recommended that investigations be initiated involving extended duration testing of the compact water electrolysis cell with wick-vapor-feed. These investigations would resolve the remaining questions relative to ultimate life and reliability. A larger capacity unit could be utilized for these tests, since the unit design may be readily scaled to any desired capacity. Minor modifications will be required in the water reservoir subassembly to provide connection to an external water supply. Many hundreds of hours have been accumulated on pre-prototype single cells of this configuration with no apparent degradation in performance.

During the additional performance testing scheduled for the electrolysis units prior to the orbital test, it is recommended that the detailed instrumentation calibrations be extended to lower temperatures. It may prove desirable to run the flight test at a lower cell temperature than the 140°F point assumed during design. A considerably lower temperature appears feasible based on the results of the Performance Acceptance Test.

It is also recommended that detailed calibrations be made on the entrainment sensors and capillary flow tubes in place on the unit. Much more precise calibrations for the normal operating environment should be feasible in this manner.

Prior to environmental testing or the actual orbital test on the units, the DC7 electrical disconnects supplied for connection to the PA 208 pressure transducers should be removed. Bendthe electrical pins into loops, supporting the pins at the base during this operation. Solder the lead wires directly to the pins and insulate as required. It is mandatory to heat sink the base of the pin during this operation in order not to damage the internal structure of the transducer by heat. A calibration re-check is advisable after this operation.

"The aeronautical and space activities of the United States shall be conducted so as to contribute . . . to the expansion of human knowledge of phenomena in the atmosphere and space. The Administration shall provide for the widest practicable and appropriate dissemination of information concerning its activities and the results thereof."

—NATIONAL AERONAUTICS AND SPACE ACT OF 1958

NASA SCIENTIFIC AND TECHNICAL PUBLICATIONS

TECHNICAL REPORTS: Scientific and technical information considered important, complete, and a lasting contribution to existing knowledge.

TECHNICAL NOTES: Information less broad in scope but nevertheless of importance as a contribution to existing knowledge.

TECHNICAL MEMORANDUMS: Information receiving limited distribution because of preliminary data, security classification, or other reasons.

CONTRACTOR REPORTS: Technical information generated in connection with a NASA contract or grant and released under NASA auspices.

TECHNICAL TRANSLATIONS: Information published in a foreign language considered to merit NASA distribution in English.

TECHNICAL REPRINTS: Information derived from NASA activities and initially published in the form of journal articles.

SPECIAL PUBLICATIONS: Information derived from or of value to NASA activities but not necessarily reporting the results of individual NASA-programmed scientific efforts. Publications include conference proceedings, monographs, data compilations, handbooks, sourcebooks, and special bibliographies.

Details on the availability of these publications may be obtained from:

SCIENTIFIC AND TECHNICAL INFORMATION DIVISION

NATIONAL AERONAUTICS AND SPACE ADMINISTRATION

Washington, D.C. 20546